# CELL VIABILITY, FUNCTIONAL AND CELL SURFACE CHARACTERISTICS OF TOOTH DERIVED STEM CELLS

Ph.D. Thesis

**Zambaga Khorolsuren**

School of Clinical Medicine

Semmelweis University

Supervisors: László Kőhidai MD, CSc and
János Vág DMD, Ph.D.

Official reviewers: Gábor Rácz Ph.D. and
Márton Kivovics DMD, Ph.D.

Head of the Final Examination Committee: †Fábián Tibor, CSc.

Members of the Final Examination Committee:
Blazsek József, Assoc. Prof. and
Vályi Péter, Assist. Prof.

Budapest

2021

*Dedicated to my Khodol*

*(Хайрт Ходолынхоо гэгээн дурсгалд зориулав.)*

**TABLE OF CONTENTS**

LIST OF ABBREVIATIONS ..... 5

1. INTRODUCTION ..... 8

1.1 Background ..... 8

1.1.1 Dental tissues are stem cell niche ..... 9

1.1.2 PDL derived stem cells (PDLSCs) ..... 11

1.2 Integrin-mediated cell adhesion ..... 12

1.2.1 RGD motif ..... 14

1.2.2 Synthetic RGD peptides ..... 15

1.3 Dental antiseptic agents ..... 17

1.3.1 Chlorhexidine (CHX) ..... 18

1.3.2 Cetylpyridinium chloride (CPC) ..... 18

1.3.3 Triclosan (TCS) ..... 18

1.3.4 Povidone-iodine (PVP-I) ..... 19

2. OBJECTIVES ..... 20

3. MATERIALS AND METHODS ..... 21

3.1 Material and methods for functional and cell surface characteristics of PDLSCs ..... 21

3.1.1 Isolation and cultivation of PDLSCs ..... 21

3.1.2 Cultures of MRC-5 and HGEP cells ..... 21

3.1.3 Preparation of adhesive coatings ..... 22

3.1.4 Adhesion and proliferation assay with impedimetric xCELLigence system ..... 22

3.1.5 Wound-healing assay (Cell migration) ..... 24

3.1.6.1 Flow cytometry analysis ..... 24

3.1.6.2 Immunofluorescence ..... 25

3.1.7 Osteogenic induction ..... 25

3.1.7.1 Alkaline phosphatase activity (ALP) ..... 25
3.1.7.2 Alizarin Red S staining (ARS) ..... 26
3.1.7.3 RNA isolation and Real-time quantitative PCR (RT-qPCR) ..... 26
3.1.8 Adipogenic Induction ..... 27
3.1.8.1 Oil Red O staining ..... 27
3.1.9 Cell differentiation monitoring: Real-Time Electrical Cell-Substrate Impedance Spectroscopy (ECIS) ..... 27
3.2 Material and methods for the viability of PDLSCs ..... 28
3.2.1 Cell seeding ..... 28
3.2.2 Preparation of antiseptic solutions and evaluation of cellular morphology ..... 28
3.2.3 Evaluation of cellular morphology ..... 29
3.2.4 Fluorescence-based alamarBlue® assay ..... 29
3.2.5 xCELLigence Real-time cell analysis (RTCA) ..... 29
3.3 Statistical analysis ..... 30
4. RESULTS ..... 31
4.1 Results for functional and cell surface characteristics of PDLSC ..... 31
4.1.1 Real-time impedimetric analysis for adhesion and proliferation of PDLSCs ..... 31
4.1.2 Wound healing assay ..... 32
4.1.3 Flow cytometry analysis ..... 34
4.1.4 Immunofluorescence staining ..... 37
4.1.5 Osteogenic differentiation capacity ..... 37
4.1.5.1 ALP activity ..... 37
4.1.5.2 Alizarin Red S staining ..... 38
4.1.5.3 Real time-qPCR ..... 40
4.1.6 Adipogenic differentiation ..... 42

4.1.7 ESIC monitoring for osteogenic and adipogenic differentiation ..... 43
4.2 The effect of anticeptics on the cell viability of PDLSCs ..... 45
4.2.1 Determination of cell numbers ..... 45
4.2.2 Cell morphology assessment ..... 46
4.2.3 Cetylpyridinium chloride (CPC) ..... 48
4.2.4 Chlorhexidine (CHX) ..... 48
4.2.5 Triclosan (TCS) ..... 51
4.2.6 Povidone iodine (PVP-I) ..... 51
5. DISCUSSION ..... 55
6. CONCLUSIONS ..... 60
7. SUMMARY ..... 61
8. ÖSSZEFOGLALÁS ..... 62
9. REFERENCES ..... 62
10. BIBLIOGRAPHY OF THE CANDIDATE ..... 78
11. ACKNOWLEDGEMENTS ..... 79

## LIST OF ABBREVIATIONS

| | |
|---|---|
| α-MEM | Minimum essential medium, α modification |
| µg/ µM/ µl | Microgram/ micromole/ microliter |
| AIM | Adipogenic induction medium |
| ALCAM | Activated leukocyte cell adhesion molecule |
| ALP | Alkaline phosphate |
| ARS | Alizarin Red S |
| BGLAP | Bone gamma-carboxy glutamic acid-containing protein (Osteocalcin) |
| BMMSC | Bone marrow mesenchymal stem cell |
| BSA | Bovine serum albumin |
| CHX | Chlorhexidine |
| CI | Cell index |
| CPC | Cetylpyridinium chloride |
| DCI | Delta cell index |
| DFPC | Dental follicle progenitor cell |
| DMEM | Dulbecco's modified eagle medium |
| DMSO | Dimethyl-sulfoxide |
| DNA | Deoxyribonucleic acid |
| DPSC | Dental pulp stem cell |
| DSC | Dental stem cell |
| ECIS | Electrical Cell-Substrate Impedance Spectroscopy |
| ECM | Extracellular matrix |
| EDTA | Ethylenediaminetetraacetic acid |

| | |
|---|---|
| FACS | Fluorescence-activated cell sorting |
| FBS | Fetal bovine serum |
| FN | Fibronectin |
| g | g-Force |
| GBR | Guided bone regeneration |
| GTR | Guided tissue regeneration |
| h | Hour |
| HGEP | Human gingival epithelial cell |
| IBSP | Integrin binding sialoprotein (Bone sialoprotein) |
| IC50 | The half-maximal inhibitory concentration |
| ICAM-1 | Intercellular adhesion molecule 1 |
| MCAM | Melanoma cell adhesion molecule |
| MFI | Mean fluorescence intensity |
| mg/ mM/ ml | Milligram/ millimole/ milliliter |
| mg/ml | Milligram per milliliter |
| MIC | Minimum inhibitory concentration |
| min | Minute |
| MRC-5 | Human lung fibroblast cell line |
| MSC | Mesenchymal stem cell |
| NCI | Normalized cell index |
| OD | Optical density |
| OIM | Osteogenic induction medium |
| Osx | Osterix |

| | |
|---|---|
| PBS | Phosphate buffered saline |
| PDL | Periodontal ligament |
| PDLC | Periodontal ligament cell |
| PDLSC | Periodontal ligament stem cells |
| PVP-I | Povidone-iodine |
| qPCR | Quantitative Polymerase Chain Reaction |
| RGD | Arginine-glycine-aspartate |
| RNA | Ribonucleic acid |
| RPLP0 | Ribosomal protein lateral stalk subunit P0 |
| RTCA | Real-time Cell Analyzer |
| RUNX2 | Runt-related transcription factor 2 |
| SC | Stem cell |
| SCAP | Stem cells from apical papilla |
| SHED | Stem cells isolated from human deciduous teeth |
| STRO-1 | Early mesenchymal stem cell marker |
| TCS | Triclosan |
| VCAM-1 | Vascular cell adhesion protein 1 |

# 1. INTRODUCTION

## 1.1 Background

The normal periodontium provides the support needed to maintain tooth function. It is composed of the gingiva, cementum, periodontal ligament (PDL), and alveolar bone. Periodontitis is a pathological inflammatory condition caused by certain bacteria in the dental plaque and affects teeth function and periodontal tissue destruction, and eventually leads to tooth loss (1). It is also linked to systemic disorders, including diabetes (2), coronary heart disease (3), dementia (4), and various types of cancers (5). The therapy of periodontal diseases generally aims i) primary and secondary prevention by controlling infection and inflammation; and ii) maintenance and improvement of the health, function, comfort, and aesthetics of all supporting structures. Over the years, the concepts in restoring damaged periodontal tissue have changed significantly, from substitution to restoration, and finally, regeneration (6) (7). The ultimate goal of periodontal therapy is to regenerate complete periodontal tissues, including the alveolar bone, cementum, and periodontal ligament (PDL) in the damaged periodontium (8).

Conventional treatments, such as root planning and scaling, can slow the progression of the disease and reduce inflammation; however, it fails to restore the tissue and bone loss (5).

Pioneering works in regenerative periodontal therapies: guided tissue regeneration (GTR) and guided bone regeneration (GBR) have been the most dynamic treatments in the past three decades. GTR is based on the theoretical principle of removing unwanted cell lines from healing sites to enable desired tissue growth (9). These approaches allow wound stabilization, space maintenance, and selective cell repopulation and have shown some effectiveness in achieving the reconstruction of intrabony components; however, clinical outcomes are highly variable and unpredictable (10–13). This regenerative potential of periodontal tissue has been attributed to the presence of undifferentiated stem cells in periodontal tissue (14).

Stem cells (SCs) have been opening a promising future in regenerative medicine because of their characteristics of self-renewal and capacity to differentiate into various types of cells (multi-potency) (15). Chronic non-healing wounds and inflammatory

conditions such as periodontitis have been hypothesized to be treated potentially by the use of SCs (16). They reside in a dynamic and specialized microenvironment represented as a niche, which is composed of heterogeneous cell types, extracellular matrix (ECM), and soluble factors (17). There are two major categories of SCs: embryonic stem cells (ESCs) and adult stem cells (ASCs).

ESCs are originated from the undifferentiated inner mass cells of a human embryo, and they can differentiate into all primary germ layers: ectoderm, endoderm, and mesoderm (18). However, ESCs are associated with huge ethical controversies and safety concerns (19).

The ASCs, also known as somatic stem cells, are undifferentiated cells found throughout the postnatal body, which regenerate damaged tissues by cell division to replace dying cells (20). The use of ASCs in regenerative medicine is considered a more achievable strategy because they are easier to isolate than ESCs, and have fewer ethical concerns (21). Adult mesenchymal stem cells (MSCs) are multipotent SCs with self-renewal potential, first isolated from bone marrow, termed as BMMSCs (22). But BMMSCs therapy has several limitations including difficulty in their isolation, complex preparation, and ethics of ways they are harvested and delivered (16). In recent years, MSCs have been identified in many different kinds of tissues and organs such as adipose tissue, bone marrow, skin, peripheral blood, cord blood tooth, etc. (23).

Since stem cell-based tissue engineering and regenerative medicine emerged in recent decades, novel therapeutic approaches have been evaluated for their capability to restore, repair, preserve, and enhance tissue-structure function. For the regenerative strategy, elements including stem cells, biomaterials, tissue-inducing substances, or biomimetic regenerative environments are essential.

### 1.1.1 Dental tissues are stem cell niche

The tooth is a multi-structured chewing organ that consists of the hard tissues of enamel, dentin, and cementum, together with the soft connective tissues, including dental pulp and the associated periodontium. Embryologically, mammalian teeth develop from interactions between oral epithelium and neural crest-derived mesenchyme (24). Dental tissues have proven to be niches for adult mesenchymal stem

cells (25). Dental stem cells (DSCs) are adult stem cell populations with MSCs characteristics, including self-renewal and multi-lineage differentiation potential (26).

Several populations of stem cells have been isolated from mature and immature teeth.
Dental pulp stem cells (DPSCs): which were the first isolated MSCs from human teeth have the potential to differentiate into odontoblasts, osteoblasts, chondrocytes, myocytes, adipocytes, and neurocytes in vitro and in vivo (27), (28).
Stem cells isolated from human exfoliated deciduous teeth (SHEDs): have differentiation patterns similar to DPSCs, but with more proliferative activity than bone marrow mesenchymal stem cells (BMMSCs) or DPSCs. It has bone/dental, cartilage, adipogenic, and neurogenic differentiation patterns similar to DPSC but has higher proliferative activity than bone marrow MSC or DPSC (29).
Periodontal ligament stem cells (PDLSCs): were identified in the periodontal ligament of extracted teeth by Seo and co-workers in 2004, and it was reported to have differentiation potential into cementoblast-like cells, adipocytes, and collagen-forming cells and showed a capacity to generate a cementum/PDL-like structure (30).
Stem cells from apical papilla (SCAP): were reported in apical papillae of the developing tooth root apex, which is thought to be associated with root formation. SCAPs have characteristics highly proliferative, migratory, and regenerative potential and can form dentin *in vivo* (31).
Dental follicle progenitor cells (DFPCs): were first isolated from the dental follicle of the human third molar and reported as the progenitor cells or precursor cells of cementoblasts, periodontal ligament cells, and osteoblasts (32).
Extracted teeth are often discarded in the clinic as medical waste and therefore present a very attractive source for SCs because of their availability. Moreover, dental SCs show immunomodulatory properties by secreting cytokines and immune receptors (26).
Due to their excellent capacity for multi-lineage differentiation, dental SCs are considered to be the potential source for tissue engineering and dental regenerative medicine.

### 1.1.2 PDL derived stem cells (PDLSCs)

Periodontal ligament (PDL) is the soft connective tissue located between the tooth root and the inner wall of the alveolar socket. It contains heterogeneous cell populations and plays a critical role in the regeneration of periodontal tissue by providing multi-potent stem cells and osteogenic progenitor cells capable of regenerating cementum, bone, and the connective tissue itself (33-36).

Since the first isolation of PDLSCs in 2004 (30), many researchers have repeated such isolations and studied the characteristics of the resulting PDLSCs. Human PDLSCs were revealed to have higher growth potential than BMMSCs and DPSCs (37), (38). The high self-renewal potential of PDLSCs was suggested to be associated with the fact that PDL tissue was continually exposed to mechanical force during mastication and the exposure of PDL cells to static mechanical strain increased their proliferation rate (39). Many other factors such as age, hypoxia condition, and signaling pathways were reported to regulate the proliferation of human PDLSCs (40).

PDLSCs have the capability to differentiate into osteogenic/cementogenic (30), adipogenic (34), chondrogenic (34), and neurogenic (41) lineages under defined conditions and exhibit an ability for immunomodulation (42), (43) while having low immunogenicity (44), (35).

Human PDLSCs were firstly identified using two early MSCs-related cell surface molecules, STRO-1 and CD146 (30), and additionally, PDLSCs express an increased level of tendon-specific transcription factors (30). For identifying MSC-like SCs, the minimal criteria for MSCs (adherence to plastic, multipotent differentiation, and positive expression CD105, CD73, and CD90 and negative expression of hematopoietic SCs) have been a gold standard (37). Numerous types of MSC- related cell surface markers such as CD10, CD13, CD26, CD29, CD44, CD71, CD73, CD90, CD105, CD106, CD146, CD166, CD349, STRO-1, STRO-3, and TNAP/MSCA-1 have been identified in PDLSC (45). However, MSC-like cells isolated from different tissues display greatly varied growth and differentiation potentials in vitro and in vivo (38), (39). Some studies indicated that human PDL tissue contains neural crest-like cells (40), (46), (47). Moreover, PDLSCs express CD271, a marker for neural crest SCs and MSCs, and it was confirmed that $CD271^{+}$ cells showed increased osteogenic potential

(48). Besides, the strong expression of ESCs pluripotency markers (OCT4 and NANOG) was also observed in human PDLSCs (49). Iwasaki et al. established that PDLSCs shared similarities with pericytes in morphology, differentiation potential, and cell phenotype (expression of CD146), and were also able to form capillary-like structures (50). However, not all the cells found within the PDL are stem cells, and it is a challenging task to identify and isolate PDLSCs in a tissue sample.

In periodontal regeneration, the attempts with cell therapy mostly have used PDL-derived stem cells because they have shown a higher potential to promote periodontal tissue regeneration compared with other tissue-derived MSCs (51). Many studies have confirmed that PDL cells can be transplanted into periodontal defects with no adverse immunologic or inflammatory consequences (52-55). Successful regenerative results were presented in experimental periodontal defects implanted with cultured PDL cells (56–58). As reported in a recent systematic review of pre-clinical studies (59), the majority of the studies showed a positive effect of PDLSCs on periodontal regeneration, (60–63).

Such advantageous features of PDL-derived cells and availability through minimally invasive procedures make them a promising candidate for the regeneration of lost/damaged periodontal tissue, and there is considerable interest in developing culture systems for the scalable expansion of PDL cells to provide a large number for use in the repair of injured tissues.

Therefore, determining the functional and cell physiological properties of PDLSC is valuable for the further development of regenerative medicine.

### 1.2 Integrin-mediated cell adhesion

The survival of adherent cells depends on cell adhesion. Failure in attachment causes apoptosis in many cell types, referred to as “anoikis” (homelessness in Greek) (65), (66). Extra-cellular matrix (ECM) plays an important role in the regulation of cell behavior and cell development through direct or indirect action (67). One of the essential roles of the ECM is to support cell attachment and signaling to the cells through adhesion receptors such as integrins (68). Integrins are cell-surface transmembrane heterodimeric receptors composed of non-covalently associated α and β subunits and bind to different proteins of the ECM such as fibronectin, laminins, and

collagens, and vitronectin (69), (70). Integrin activation initiates multiple intracellular signaling pathways and leads to the regulation of cell functions such as motility, proliferation, and differentiation.

The principal integrin-binding domain in ECM proteins is the three amino acid sequence arginine-glycine-aspartate (RGD) sequence (71). Different integrin affinity of RGD loops is mainly affected by their conformation and neighboring amino acids in the respective ECM proteins (72). The unique binding of the extracellular domains of integrins to ligands induces structural and signaling changes within the cell (73). These are based on the linkage of activated integrins to the intracellular cytoskeleton through its cytoplasmic tails and enable the bi-directional transmission of signals across the cell membrane (74).

Integrin-mediated cell adhesion consists of four different partly overlapping steps: cell attachment, cell spreading, organization of actin cytoskeleton, and formation of focal adhesions (75). During these steps of cell adhesion, integrins play a role not only in physical anchoring processes but also in signal transduction through the cell membrane. Firstly, the cell contacts the surface and some ligand binding occur, which allows the cell to resist gentle shear forces. Secondly, the cell body starts to flatten, and its plasma membrane spreads over the substratum. Thirdly, this leads to actin organization into microfilament bundles, which are also called stress fibres. The fourth step is the formation of the focal adhesions, which link the ECM to actin cytoskeleton components (76) (Figure 1). Focal adhesions play a role in the organization of the actin cytoskeleton and mediate transmembrane signaling (77).

Integrins signal in two directions: ligand-binding function of integrin is regulated by “inside-out’ signaling, while “outside-in” signaling determines cellular responses induced by ligands such as migration, survival, differentiation, and motility (78). In bent form: integrin has a low affinity for ligands. Inside-out signaling: intracellular activator binds to the β-subunit, and induces affinity for ligands to regulate adhesion, migration, and spreading. Outside-in signaling: integrin binds to ligand to regulate cell polarity, survival, migration, changes in cytoskeleton, and gene expression. Unligated integrins can induce apoptosis.

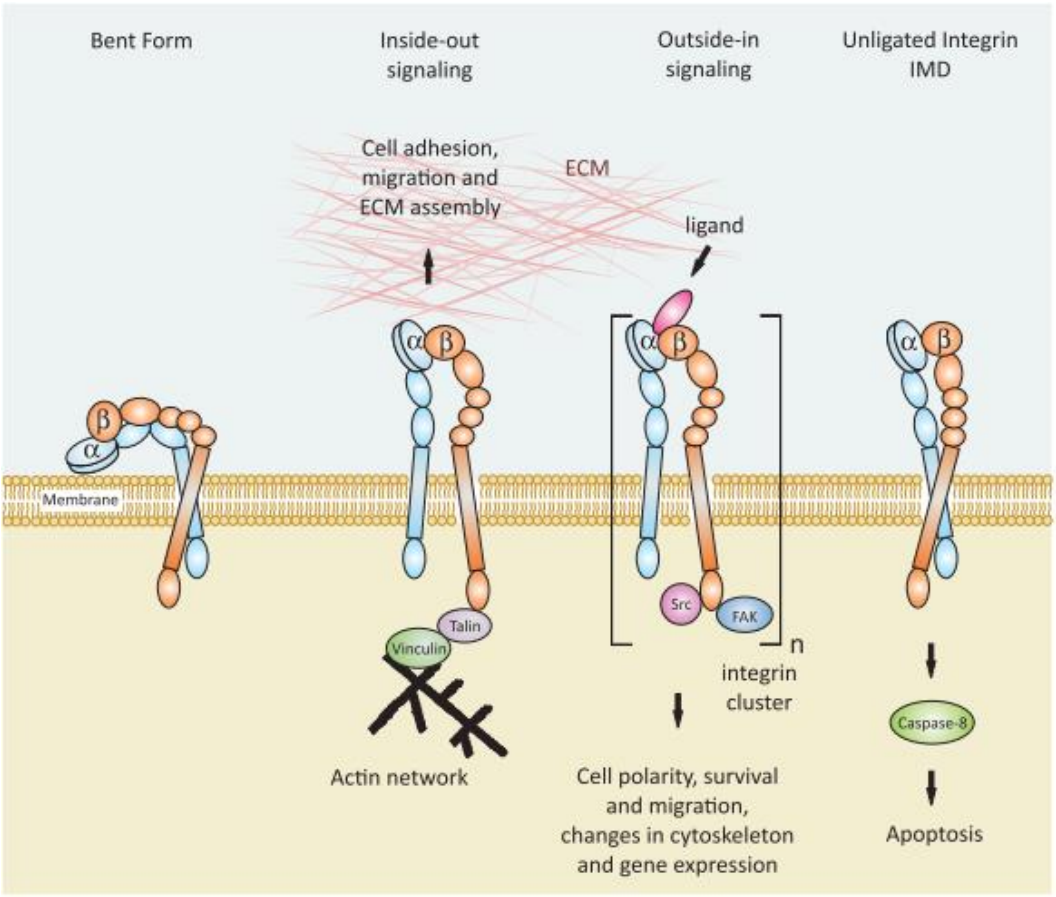


**Figure 1 Schematic representation of integrin activation and signaling mechanisms** (Mas-Moruno, Rechenmacher, and Kessler 2011) [73].

### 1.2.1 RGD motif

Arginine-glycine-aspartate (RGD) sequence was first discovered in fibronectin by Pierschbacher and Ruoslahti in 1984 (79), and its attachment promoting activity was soon confirmed (80), and extended to be found in many other adhesive proteins of ECM such as vitronectin, osteopontin, laminin, etc. (81), (71). Subsequently, integrins, the cell surface receptors that recognize the RGD sequence of ECM proteins were discovered (82), and it has been confirmed that the RGD sequence can bind to multiple integrin types (83).

The application of RGD motifs has been studied in different fields including drug delivery, diagnostics, theranostics, and tissue engineering. It is commonly established as

a target for imaging agents, drugs, gene delivery for tumor treatment to deliver therapeutic or diagnostic agents into cancerous cells, platelets, etc., which overexpressed certain integrin receptors on their surface (84). Recently, there have been various clinical trials regarding RGD peptides diagnostic and drug delivery applications for several diseases (84). Furthermore, the feature that RGD can promote cell attachment to the matrix, avoid cell apoptosis and enhance new tissue regeneration makes it a very promising constitution for biomimetic materials (85).

### 1.2.2 Synthetic RGD peptides

Synthetic RGD peptides can mimic natural adhesive proteins in two ways: in solution, RGD peptides prevent adhesion, whereas when coated onto a surface, they promote cell adhesion (71). Functionalizing synthetic polymers to obtain specific cell-surface interactions is of great interest in many fields, including medicine, material science, surface engineering, chemistry, physics, biology, and biochemistry. In regenerative medicine and tissue engineering, biocompatible material to provide proper cell adherence and promote cell growth is valuable. Immobilizing RGD on the artificial surface is one approach for biomimetic surface modification. Previous study results suggest that RGD promotes cell attachment and enhances other vital cell functions and supports tissue regeneration (84) (85).

In biomedical applications, native ECM proteins have some disadvantages, such as the risk of infection, immune reactivity, and not being suitable for long-time application due to proteolytic degradation (86). Besides, compared with native ECM proteins, synthetic biomimetic RGD sequences containing short peptides are highly stable, chemically defined, and are relatively inexpensive to produce and minimize the risk of immune reactivity or pathogen transfer (87-89).

In this study, we evaluated three different RGD peptides immobilized with a poly L-lysine backbone. Poly L-lysine is a synthetic polycationic amino acid polymer, widely used for coating cell culture dishes because of its positive charge that increases cell adherence (90). Prof. Gábor Mező (MTA-ELTE Research Group of Peptide Chemistry, Budapest) kindly provided us with three different synthesized conjugates, each containing RGD sequences.

Cyclization of RGD increase stability and make them less susceptible to chemical and enzymatic degradation (91) and is considered as high affinity to cell surface integrins due to its three-dimensional structure (71). In 2008, Prof. Mező and his colleagues designed a new synthetic polypeptide composed of poly(L-lysine) backbone with oligo DL-alanine side chains (AK) carrying -cyclo[RGDfC] on the N-terminal; refers to AK-c[RGDfC]. This polypeptide conjugate was promoting serum-free early attachment of anchorage-dependent cells (92) and using its adhesive property, isolation of neural stem/progenitor cell was successful under serum-free condition (93) (Figure 2; Figure 3-A).

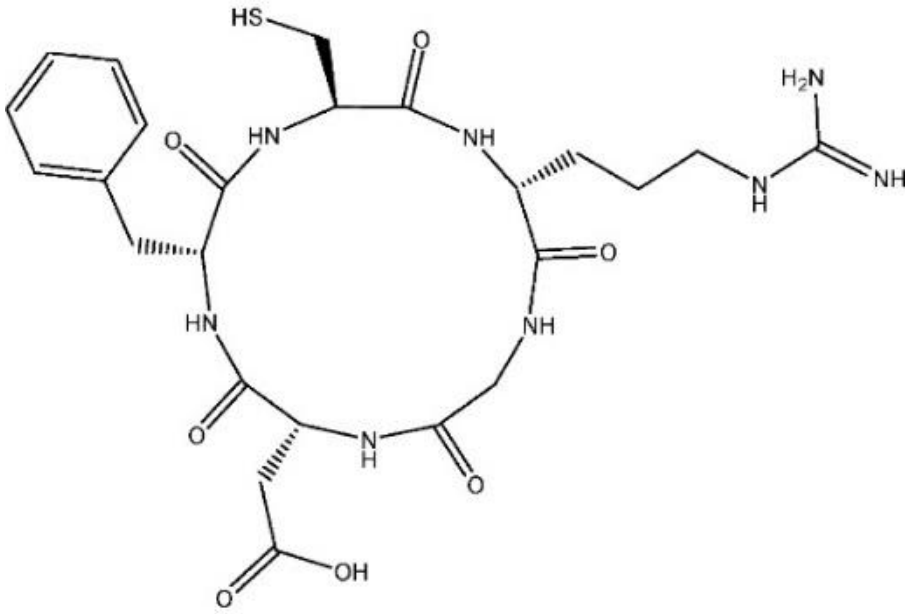


**Figure 2 Structure of cyclo[RGDfC]** (K. Marko et al. 2008) [80]

The next synthetic conjugate SAK-c[RGDfC], was synthesized based on the previous technique (92). RGD-containing pentapeptide c[RGDfC] was covalently linked to a backbone termed SAK, consisting of Poly-L-lysine with Serine-oligo-DL-alanine branches. This conjugate was previously tested with adipose tissue-derived MSCs on

the bone-implant surface and confirmed to it improve serum-free adhesion (94) (Figure 3-B).

And a third conjugate is SAK-osteopontin (SAK-opn). SAK backbone conjugated with linear osteopontin derivative (Ac-GRGDSVVYGLR-$NH_2$) (Figure 3-C).

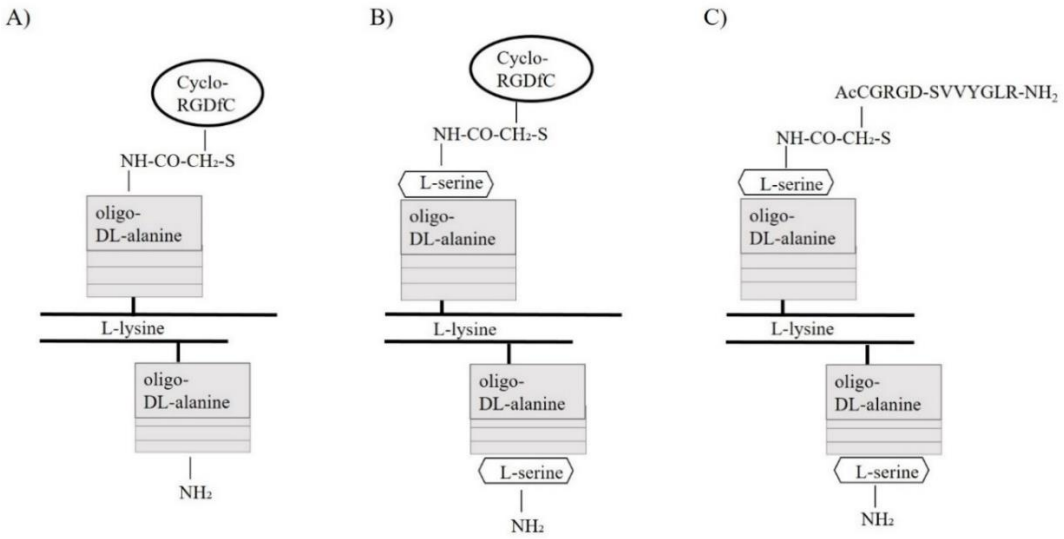


**Figure 3 Schematic representation of synthetic RGD conjugates.**

**A)** AK-c[RGDfC], **B)** SAK-c[RGDfC], and **C)** SAK-opn

### 1.3 Dental antiseptic agents

Dental antiseptics prevent or arrest the growth or action of microorganisms after topical administration. Preferably, antiseptics should have a broad spectrum with rapid onset and long-lasting effects and should not be toxic to host tissues/cells as far as possible, and they should not impair healing processes (95). Yet, studies show that commercially-available dental antiseptic products have been demonstrated to exhibit a cytotoxic effect on various cell types such as epithelial cells of buccal mucosa (96), and gingival fibroblasts (97-99), osteoblast precursor cells (100), (101). During or after dental procedures such as tooth extraction, surgical periodontal therapies, and root canal treatment, there are great chances of dental SCs to expose to antiseptics. However, very few studies have been indicated, particularly on dental SCs viability when exposed to

dental antiseptic materials. We chose to examine commonly used four different types of dental antiseptic compounds and how they affect the viability of PDLSCs.

### 1.3.1 Chlorhexidine (CHX)

CHX is a synthetic cationic bis-biguanide that has a broad spectrum against Gram-negative and Gram-positive bacteria as well as fungi and is the most widely used antimicrobial since 1958 (102). It interacts with a negatively charged surface of a microorganisms membrane (103). In dental practice, CHX has been formulated in products such as mouthwash, toothpaste, root canal irrigation solutions, etc., in a wide range of concentrations of 1-50 mg/ml (104).

### 1.3.2 Cetylpyridinium chloride (CPC)

A plaque inhibiting effect of the cationic quaternary compound cetylpyridinium chloride (CPC) was first described by Schroeder et al. in 1962 (105) and is a broad-spectrum antiseptic agent against Gram-negative and Gram-positive bacteria. The evidence suggests that CPC disturbs bacterial membrane function and collapses intercellular stability (106). It is commonly added at 0.45-0.7 mg/ml in dental mouth rinses and is effective in preventing the development of dental plaque and reducing gingivitis (107-109).

### 1.3.3 Triclosan (TCS)

Triclosan (TCS) is a commonly used antimicrobial and antifungal phenolic compound and is found in many formulations of personal care products, household items, medical devices, toys, plastic materials, and textiles, as well as dental hygiene products (110), (111). The antimicrobial mechanism of TCS is due to its hydrophobic and lipophobic characteristics, and TCS adsorbs to the lipid components of the cell membrane (112). Because of potential health concerns, for instance, antimicrobial resistance and endocrine disruption, it has been under review for decades. In 2016, the United States Food and Drug Administration (FDA) banned the inclusion of triclosan from household soap products due to its health and concerning environmental effects (113). Although, it

is available in some dental products such as mouthwash and toothpaste, mostly with a 3 mg/ml concentration.

### 1.3.4 Povidone-iodine (PVP-I)

Povidone-iodine (PVP-I) is the most widely used iodophor with a broad spectrum against bacteria, mycobacteria, fungi, viruses, and protozoa (114), (115). It affects bacterial cell walls and membranes and causes loss of cytoplasmic material and deactivation of enzymes (114). Concentration ranges of PVP-I between 0.5 – 10 mg/ml are generally used in oral hygiene and dental treatments.

## 2. OBJECTIVES

The primary purpose of this Ph.D. research project was to evaluate the human PDLSCs characteristics and responses to different materials, including novel biomimetic peptides and dental antiseptic compounds widely used in dental procedures.

1. We examined the functional and cell surface characteristics of PDLSCs. And our collaborators have synthesized integrin-binding RGD sequence containing adhesive peptides. We set our objectives to analyze:
    - adhesion and proliferation
    - migration
    - differentiation and
    - cell surface molecules of PDLSCs when cultivated on synthetic RGD peptide coatings
2. We aimed to study the cell viability of PDLSCs when exposed to dental antiseptic agents.

    Assayed antiseptic compounds are:
    - cetylpyridinium chloride
    - chlorhexidine
    - triclosan and
    - povidone-iodine

# 3. MATERIALS AND METHODS

## 3.1 Material and methods for functional and cell surface characteristics of PDLSCs

### 3.1.1 Isolation and cultivation of PDLSCs

Impacted third molars were surgically removed from 34 healthy young adults at the Department of Oral Diagnostics, Faculty of Dentistry, Semmelweis University. The procedure was performed with the permission of the Semmelweis University Regional and Institutional Committee of Science and Research Ethics:17458/2012/EKU.

Isolation of PDLSCs was done based on previously developed protocol (41) with minor modifications. Tooth surfaces were cleaned and the periodontal tissue was removed from the middle-third of the root with a sterile scalpel and digested in collagenase type I (1 mg/ ml, Gibco/ Thermo Fisher Scientific) solution dissolved in phosphate buffer saline (PBS, Lonza Group Ltd.) for 1 hour at 37°C. Then undissolved tissue parts were pushed through a 22-G needle to loosen the tissue structure and obtain a single-cell suspension. The single-cell cultures from different individuals were maintained independently under standard conditions (37 ˚C, 5% $CO_2$, 100% humidity) in the alpha modification of Eagle's medium (αMEM) (Lonza Group Ltd.) supplemented with 10% fetal bovine serum (FBS) (Gibco/ Thermo Fisher Scientific), 1% penicillin/ streptomycin (Gibco/ Thermo Fisher Scientific), and 1% glutamine (Gibco/ Thermo Fisher Scientific); but was not supplemented with L-ascorbic acid 2-phosphate. Cell cultures were passaged with 0.25% trypsin-EDTA solution (Gibco/ Thermo Fisher Scientific) when they reached 70% confluence, and passages between 2 and 5 were used for experiments.

### 3.1.2 Cultures of MRC-5 and HGEP cells

Human lung derived fibroblast cell line MRC-5 (Sigma-Aldrich) was cultured in Dulbecco's Modified Eagle's Medium (DMEM) (Sigma-Aldrich) containing 10% FBS (Gibco/ Thermo Fisher Scientific), 2 mM L-glutamine (Gibco/ Thermo Fisher Scientific), 100 µg/ml penicillin/streptomycin (Lonza Group Ltd.) and 1% non-essential amino acids (Gibco/ Thermo Fisher Scientific) and passage numbers under 35 were used in the experiment. The human gingival epithelial cell line (HGEP) (CELLnTEC)

was cultured in a CnT-24 medium (CELLnTEC) containing 1% L-glutamine and supplemented with 1% penicillin-streptomycin (Lonza Group Ltd.).

### 3.1.3 Preparation of adhesive coatings

The peptide constructs were synthesized at the MTA-ELTE Research Group of Peptide Chemistry (Budapest, Hungary). Human plasma fibronectin (FN, 1 mg/ml, Millipore) was used as a referent coating. Stock solutions for synthetic peptides 2mg/ml (AK-c[RGDfC], SAK-c[RGDfC], and SAK-opn) and human plasma FN 1mg/ml were stored at -20°C. Just before use, they were dissolved in d.i. water and cell culture plastic dishes or impedimetric arrays were coated with 10 μg/ml RGD-synthetic peptides or 16 μg/ml FN (e.g., 50 μl, 200 μl, 400 μl, and 1 ml for 96-, 24-, 12-well plate and 35 mm tissue culture dishes, respectively). The solution was left on the surface at room temperature for 1 hour, then aspirated and dried under sterile airflow for 5 minutes. The estimated surface density of the molecules was 1 $\mu g/cm^2$. The control remained uncoated.

### 3.1.4 Adhesion and proliferation assay with impedimetric xCELLigence system

Impedance-based real-time xCELLigence SP (Roche Applied Science) system was utilized for monitoring cell adhesion and proliferation. This system consists of four main components: i) an RTCA SP station that fits inside a standard tissue-culture incubator, ii) an RTCA impedance analyzer, iii) disposable E-plate 96 with gold microelectrode arrays that cover 80% of the bottom of each well, and iv) the RTCA computer with integrated software (Figure 4-A). Measuring the electronic impedance of the sensor electrodes allows for the monitoring of physiological changes in the cells. Cell viability, cell number, cell morphology, and degree of adhesion all affect electrode impedance. During the RTCA measurement, the voltage applied to the electrodes is about 20mV, which does not affect the health and behavior of the cells. In the absence of cells, electrode impedance depends primarily on the ionic environment both at the electrode and solution interface and in the bulk solution. In the presence of cells, cells attached to the electrode sensor surfaces will act as insulators and thereby alter the local ionic environment at the electrode/solution interface and cause increased impedance. Therefore, the more cells there are on the electrode, the more significant the change in

electrode impedance (116). The RTCA software calculated it as a unit-less parameter termed cell index (CI) using the following formula:

$CI = (Z_i - Z_0)/ F_i$

where $Z_i$ is the impedance at a given time point of the measurement, $Z_0$ is the impedance at the first time point of the measurement, while $F_i$ is a constant coefficient to the system depending on the frequency of alternating current (F10kHz = 15). The change in impedance from the time point immediately after cells were added onto the electrodes refer to as delta cell index (DCI).

As described above, the 96-well E-plate was pretreated with synthetic RGD peptides or FN separately. The background value was recorded for 1 hour with 100 µl standard culture medium supplemented with 10% fetal bovine (+FBS) or without FBS (-FBS), respectively. Then, $5 \times 10^3$ PDLSCs were seeded in 100 µl culture medium (+FBS or −FBS, respectively) into each well and incubated for 3 days at 37°C in 5% $CO_2$. The impedance was measured every 1 minute in the initial 24 hours, then at every 15 minutes for the rest of the time up to 96 hours. Each data point represents a mean ± SEM of three parallels. Data were analyzed by RTCA 2.0 (Roche Applied Science) of xCELLigence SP (Figure 4).

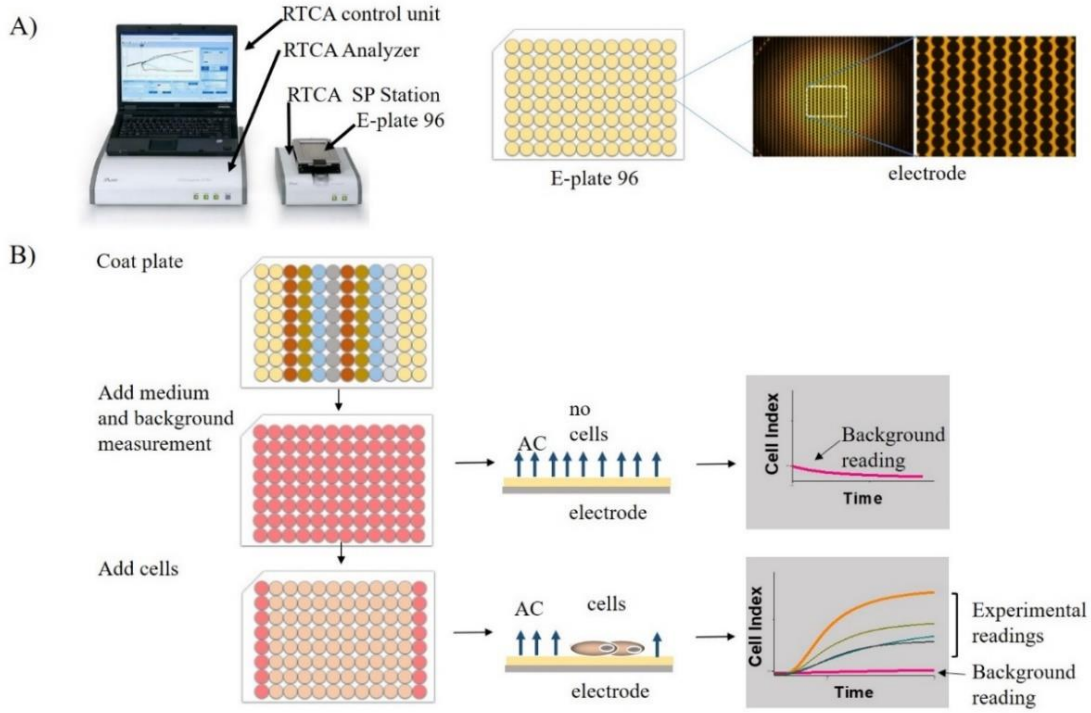


**Figure 4 The xCELLigence RTCA system for cell adhesion monitoring.**

**A)** RTCA system structure. **B)** Workflow of adhesion assay

### 3.1.5 Wound-healing assay (Cell migration)

ibidi® Culture-Insert chamber (ibidi GmbH) is a silicone insert with defined cell-free gaps. The chamber was set onto the 35 mm pre-coated or uncoated plastic dish (Thermo Fisher Scientific), and 70 µl cell suspension with $5 \times 10^5$ cells were added into each well of the chamber and incubated under standard conditions and was removed after 24 hours resulting in approximately 500 µm wide cell-free gap. The cell migration through the gap was monitored over the next 48 hours, and images were captured at different time points using Axio Observer A1 inverted microscope (Zeiss) and were evaluated by AxioVision 4.2 software. The wound area at every measured time point was normalized to the wound area at zero hour and shown in %.

### 3.1.6.1 Flow cytometry analysis

The monoclonal antibodies against to MSCs representative markers: CD146 (MCAM), CD90 (Thy-1), CD73, CD271, CD105 (endoglin), and STRO-1; integrin subunits: CD49b (integrin α2), CD49c (integrin α3), CD49d (integrin α4), CD29 (integrin β1), integrin β7 and against integrin αVβ3; other cell adhesion molecules: CD106 (VCAM-1), CD166 (ALCAM) and CD54 (ICAM-1) were used to assess the cell surface antigens of PDLSCs. Antibodies were purchased from R&D Systems, Becton-Dickinson Pharmingen, and BioLegend. Cells were seeded $5 \times 10^4$ per well into peptide-coated or uncoated 35 mm culture dishes, in standard medium and incubated at 37°C in 5% $CO_2$. Flow cytometry (FACSCalibur, Becton-Dickinson) analysis was performed after 1-day or 1-week of cultivation of PDLSCs on the coated surfaces. The cells were removed with trypsin EDTA and centrifuged at 800 × g for 5 minutes and fixed in 400 µl of 4% formaldehyde in PBS. After washing, cells were resuspended in 100 µl PBS with 1% (w/v) BSA, and 5 µl of Human TruStain FcX™ (BioLegend) was added for blocking of nonspecific Fc receptors, incubated for 10 minutes at room temperature in dark. Then added 10 µl of antibody against the specific surface molecule and incubated for 30 minutes at 2-8°C. Cells were washed with PBS and resuspended in 400 µl of PBS for final flow cytometry analysis. Data were analyzed by Flowing software (Turku Centre for Biotechnology, Finland).

#### 3.1.6.2 Immunofluorescence

Slides with attached cells were rinsed three times with PBS and fixed in 4% formaldehyde / PBS for 10 minutes at room temperature. Cells were permeabilized in 0.1% Triton X-100 dilution in PBS for 10 min and washed three times with PBS. Then, unspecific binding sites were blocked with 1% bovine serum albumin / PBS for 1 hour. MSCs markers STRO-1 and CD90 (FITC-labeled) were detected with primary antibodies respectively (for $5 \times 10^5$ cells 2.5 µl antibody in 200 µl PBS) and incubated overnight at 4°C. Washing steps (PBS, 3 times) were followed by nuclear staining with DAPI for 3 min at room temperature. After three washes with PBS, immersion oil was dropped and visualized with Zeiss Axiophot fluorescence microscopy and ZEN Blue 2.6 software (Zeiss).

### 3.1.7 Osteogenic induction

Osteogenic induction was done similarly as in the previous study (117), with minor modifications. Briefly, $4 \times 10^4$ cells/per well were seeded into a 12-well plate. Cells were cultured on RGD peptide-coated or uncoated plates in the standard medium for 48 hours. Next, the medium was aspirated, the fresh standard medium was added into control, and osteogenic inducing medium (OIM) was added to osteo-inducing cells. OIM consists of DMEM with 1.0 g/L glucose (Lonza Group Ltd.) supplemented with 10% FBS, 1% penicillin/streptomycin, and 1% glutamine, containing 0.1 mM L-ascorbic acid 2-phosphate (Sigma-Aldrich), 10 mM β-glycerophosphate (Sigma-Aldrich), and 10 nM dexamethasone (Tocris Bioscience). The cells were incubated at 37°C in 5% $CO_2$. The media were refreshed every 2-3 days.

#### 3.1.7.1 Alkaline phosphatase activity (ALP)

ALP assay was performed after one and two weeks post osteogenic induction. Media were aspirated, and cells were washed twice with PBS 400 µl/well. Then 200 µl of 14% 2-amino-2 methyl-1 propanol (AMP) buffer (Sigma-Aldrich) and 200 µl of Alkaline Phosphatase Yellow (pNPP) Lipid Substrate System for ELISA (Sigma-Aldrich) were added into each well. After 20 minutes at 37°C, the suspension was mixed by pipette,

and 200 µl from each sample was transferred into a 96-well plate, and optical density (OD) was measured at 405 nm single wavelength by LabSystems Multiscan MS reader (Thermo Fisher Scientific).

#### 3.1.7.2 Alizarin Red S staining (ARS)

Alizarin Red S (ARS) staining was performed 1, 2, and 3-weeks post-induction. Cells were fixed with 400 µl of 10% formaldehyde for 30 minutes, then washed with PBS twice. Then, 2% ARS solution 400 µl per well was added and was incubated at room temperature for 15 minutes. After that, suspensions were aspirated, and cells were washed with distilled water. Cell staining was observed under light microscopy, and photographs were taken. To define the quantitative value of optical density, we followed a previously established protocol (118). Briefly, 400 µl of 10% acetic acid was added per well and incubated for 30 minutes. Then cell layers were gently scraped and transferred with the acetic acid into a micro-tube and vortexed well. After being heated at 85°C for 10 minutes, cooled on ice, and centrifuged at 20.000 g. The supernatant was transferred to a 96-well plate, and the OD value was measured with LabSystems Multiscan MS (Thermo Fisher Scientific) reader at the 405 nm single wavelength.

#### 3.1.7.3 RNA isolation and Real-time quantitative PCR (RT-qPCR)

Total RNA was extracted from harvested cells using GeneJet RNA Purification kit (Applied Biosystems/ Thermo Fisher Scientific) two weeks post osteogenic induction. Contaminant DNA removal was done with RapidOut DNA Removal Kit (Applied Biosystems/ Thermo Fisher Scientific). A reverse transcription reaction was performed with Maxima First Strand cDNA Synthesis Kit (Applied Biosystems/ Thermo Fisher Scientific) according to the manufacturer's instruction: 3 µg of total RNA was used in 20 µl final volume. Quantitative real-time PCR was performed with StepOne™ Real-Time PCR System (Applied Biosystems/ Thermo Fisher Scientific) with the default setting (50°C for 2 min, 95°C for 10 min, 45 cycles: 95°C for 15 s, 60°C for 1 min) and TaqMan® Universal Master Mix II (Applied Biosystems/ Thermo Fisher Scientific) assay. The procedure was done following the manufacturer's instructions. Briefly, 1 µl aliquot of cDNA was used in a final volume of the 20 µl reaction mixture, which contains 1 µl of TaqMan® primers. The primers for osteoblast-related genes were

purchased from Applied Biosystems/ Thermo Fisher Scientific: Alkaline phosphatase (ALPL) (Hs 01029144_m1), Runt-related transcription factor (RUNX2) (Hs 00231692_m1), Bone sialoprotein (IBSP) (Hs 00173720_m1), bone-specific transcription factor-osterix (SP7) (Hs 01866874_s1) and Osteocalcin (BGLAP) (Hs 01587814_g1). And human acidic ribosomal phosphoprotein P0 (RPLP0) (Hs99999902_m1) was used as an internal control gene. Data were analyzed by StepOne 2.2.2 Software.

### 3.1.8 Adipogenic Induction

PDLSCs were seeded ($2 \times 10^5$) into a 6-well plate in a standard medium. Similarly, to an earlier study (119), two days later, the standard medium was replaced by an adipogenic induction medium (AIM) consisting of DMEM with 1.0 g/L glucose without L-Glutamine supplemented with 10% FBS, 1% penicillin/streptomycin, and 1% glutamine, 0.5 µM dexamethasone (Tocris Bioscience) and 0.5 mM 3-isobutyl-1-methylxanthine (IBMX) (Sigma-Aldrich) and 50 µM indomethacin (Sigma-Aldrich).

#### 3.1.8.1 Oil Red O staining

After 14 and 21 days of adipogenic induction, cytoplasmic lipid droplets were visualized by Oil Red O staining. Briefly, 0.5% Oil Red O solution was prepared in 100% isopropanol and filtered with a 0.2 µm filter syringe. Cells were fixed with 10% phosphate-buffered formaldehyde for 30 minutes at room temperature and aspirated. Cells were rinsed with PBS, and 50 µl of Oil Red O staining solution was added. After 15 minutes of incubation at room temperature, cells were washed with distilled water and observed under a light microscope, and photographs were taken.

### 3.1.9 Cell differentiation monitoring: Real-Time Electrical Cell-Substrate Impedance Spectroscopy (ECIS)

The electric cell-substrate impedance sensing (ECIS) technique was pioneered by Giaever and Keese (120). ECIS applies a very weak (<1µA), noninvasive AC to cells seeded on a gold electrode array, allowing the cell impedance current to be monitored in

real-time (121). It measures the complex impedance spectrum (Z, R, C) and evaluates dynamic aspects of cultured cells through their dielectric properties.

In this study, we utilized ECIS® Zθ (Applied BioPhysics) instrument to track PDLSCs undergoing osteogenic and adipogenic differentiation and to evaluate whether the synthetic RGD peptides affect cell behavior during the differentiation processes. We used a 96W1E plate which has 2 electrode arrays per well. Before the measurement, the plate surface was stained with synthetic peptides and dried as described above. The plate was conditioned with 10 mM cysteine 200 µl per well and incubated at room temperature for 1 hour. After that, the cysteine solution was aspirated, and the surface was coated with synthetic RGD peptides, as described above. A baseline measurement was run with 100 µl standard medium for 1 hour. Next, $1 \times 10^4$ cells/well were seeded in 100 µl medium and incubated at 37°C in 5% $CO_2$. After 48 hours of incubation, the standard medium was replaced with 200 µl OIM or AIM respectively. Measurements were taken every 10 minutes at frequencies ranging from 1 kHz to 64 kHz and continued for up to two weeks. Media were refreshed every 2-3 days.

### 3.2 Material and methods for the viability of PDLSCs

#### 3.2.1 Cell seeding

For the alamarBlue® assay, PDLSCs were seeded $10^4$ per well with 200 µl culture media into a 96-well culture plate. The cells were incubated at 37°C in 5% $CO_2$ for 24 hours to allow cell adhesion. For impedimetric xCELLigence analysis, 100 µl of cell culture media was added into each well of an E-96 plate and baseline impedance was determined at 37°C. After about 1-hour of baseline impedance recording, $10^4$ cells/well were seeded into each well with 100 µl culture media.

#### 3.2.2 Preparation of antiseptic solutions and evaluation of cellular morphology

Stock solutions of cetylpyridinium chloride (CPC), chlorhexidine (CHX) and povidone-iodine (PVP-I) were solubilized in d.i water and triclosan (TCS) was solubilized in dimethyl sulfoxide (DMSO); and appropriate dilutions of 22 µl was added per well in 96-well plate cultures. Final concentrations were: CPC (Sigma-Aldrich) 0.0001, 0.001,

0.01 and 0.1 mg/ml; CHX (Sigma-Aldrich) 0.001, 0.01, 0.1 and 1 mg/ml; TCS (Sigma-Aldrich) 0.01, 0.1, 1 and 2 mg/ml; and PVP-I (Abcam) 0.1, 1, 2 and 4 mg/ml. Controls received d.i water or ×100 times dilution of DMSO regarding solvents.

### 3.2.3 Evaluation of cellular morphology

Cells were incubated with different concentrations of antiseptic agents for 24 h, and the cell morphology was examined by an inverted microscope Axio Observer A1 (Zeiss).

### 3.2.4 Fluorescence-based alamarBlue® assay

The biochemical procedure of the alamarBlue® assay is based on cell-permeable and non-toxic weakly fluorescent blue indicator dye called resazurin (7-Hydroxy-3H-phenoxazin 3-one 10-oxide), which becomes highly fluorescent when reduced by oxidoreductases within viable cells. The alamar blue solution was prepared with 0.15 mg/ml resazurin sodium salt (Sigma-Aldrich) in phosphate-buffered saline (PBS). After 24 h of cell attachment, 22 µl/well antiseptic agents were added with a range of concentrations and incubated for ultra-short term:10, 20, 30 seconds; short term: 10, 20, 30 minutes; and long term: 24 and 48 hours, at 37°C in a 5% $CO_2$. After the incubation, all fluids were aspirated and washed with PBS then the fresh medium was added to 200 µl/well. Next, alamar blue solution was added to 25 µl/well, and cells were incubated at 37°C, protected from light for 6 hours. Fluorescence intensity was measured with a Spectrophotometer at wavelength 565; 590 nm.

### 3.2.5 xCELLigence Real-time cell analysis (RTCA)

Real-time xCELLigence SP (Roche Applied Science) system was used for monitoring cytotoxicity and cell proliferation of PDL cells under stimuli of antiseptic agents for the ultra-short, short and long term. Cells were grown before the experiment for 24 hours in an incubator at 37°C in 5% $CO_2$. Subsequently, 22 µl antiseptic solutions were added to each well. Ultra-short-term monitoring was applied for a 1-minute duration and recorded every 1 second, and long-term monitoring was done for 48 hours, recorded

every 1 minute for the first 24 hours and every 15 minutes for the rest of the time. xCELLigence system is based on electronic impedance reading from the gold plated sensor electrodes that are fused to the bottom of the plates and represented by cell index (CI). When there is an absence of living cells or suspension of dead cells, the CI value is close to zero (122). Data were plotted as the normalized cell index (NCI), which is the cell index for the given time point divided into cell index immediately before compound addition time. Data were evaluated with RTCA 2.0 software (Roche Applied Science).

### 3.3 Statistical analysis

Each experiment was performed with PDLSC cultures derived from at least three different patients. In the case of each donor sample, 2-4 parallel measurements were performed for each experimental group. For the xCELLigence measurement cell index (CI), normalized cell index (NCI), cell index slope, and half-maximal inhibitory concentration (IC50) value for xCELLigence measurement were calculated automatically by the RTCA 2.0 software. The IC50 value from the alamarBlue® assay was calculated using nonlinear regression by OriginPro 8.5 (OriginLab Corporation) software. Data are expressed as mean ± standard errors of the mean from at least three independent experiments. A p-value of $<0.05$ was considered significant. Statistical evaluation of the data was carried out by Origin 8.5 software applying one-way ANOVA + Tukey and Bonferroni test.

# 4. RESULTS

## 4.1 Results for functional and cell surface characteristics of PDLSC

### 4.1.1 Real-time impedimetric analysis for adhesion and proliferation of PDLSCs

The electrode surfaces were pre-coated with human plasma fibronectin (FN), synthetic SAK-c[RGDfC], AK-c[RGDfC], and SAK-opn. Cells were cultured under two different conditions: medium supplemented or not with 10% FBS (+FBS and –FBS, respectively). Adhesion and proliferation of PDLSCs were monitored over 96 hours.

The DCI curve reveals the initial phase of cell adhesion and spreading (approximately 0–8 h), followed by a plateau phase (approximately 8-40 h) before a gradual period of proliferation (since approximately 40 h) in +FBS culture (Figure 5-A). Cell adhesion was quantified as slope value (the rise of a line laid on a defined interval of the curve) (1/h) calculated by RTCA software. Under +FBS conditions, cell adhesion slope in the first hour was significantly increased in all experimental groups compared with control; then 0-4 h slope shows SAK-opn was not considerably active compared with control (Figure 5-B).

When FBS was absent from the growth medium, cell adhesion was significantly induced by cyclic RGD peptides in the first hour, while the linear SAK-opn peptide effect was not significantly different compared with control uncoated (Figure 5-C, Figure 5-D). After cell adhesion was completed 0- 8 h, the NCI curve remained steady in –FBS culture.

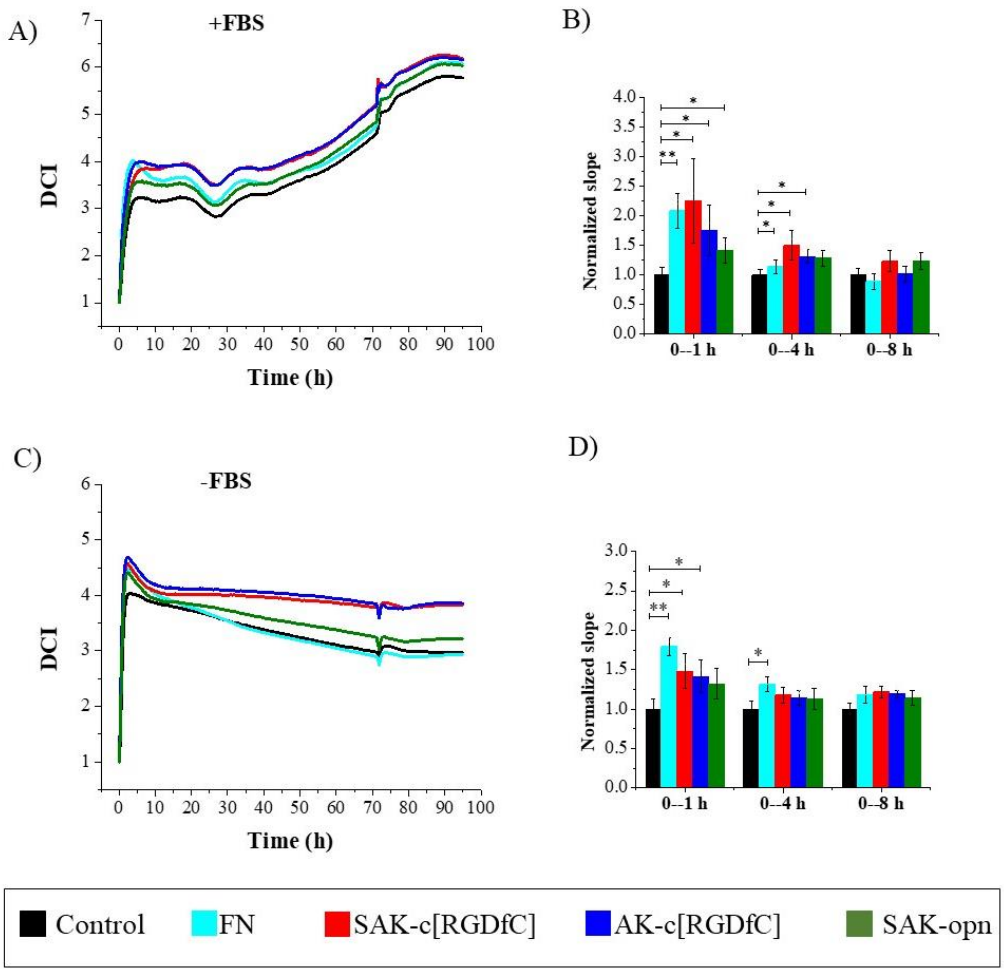


**Figure 5 Impedimetric RTCA analysis for adhesion and proliferation of PDLSC**. The representative curve graphs describe the delta cell index (DCI) plotted against time. Cells were seeded onto peptide-coated surfaces and cultured in **A)** 10% fetal bovine serum (+FBS) containing medium; **C)** absence of serum in medium (-FBS). Bar graphs show dynamic changes in adhesion **B)** +FBS culture; **D)** –FBS culture. Data are presented as mean ± standard error (SEM) from 3 independent experiments. Statistical differences compared with control $^{*}p \leq 0.05$; $^{**}p \leq 0.01$.

### 4.1.2 Wound healing assay

Cell-free 500µm gap/wound was created using ibidi® Culture-Insert chamber on peptide pre-coated plastic ware or uncoated control (Figure 6-A). The wound size immediately after the chamber removal was taken as 100%. After 24 hours, the wound area was reduced to 25.6% on AK-c[RGDfC], 36.2% on SAK-c[RGDfC], 39.6% on FN

coatings; while it was 52.3% on SAK-opn coating, which was similar to uncoated control (56.5%) (Figure 6-B). After 48 h, the wound area was completely occupied by the cells.

**A)**

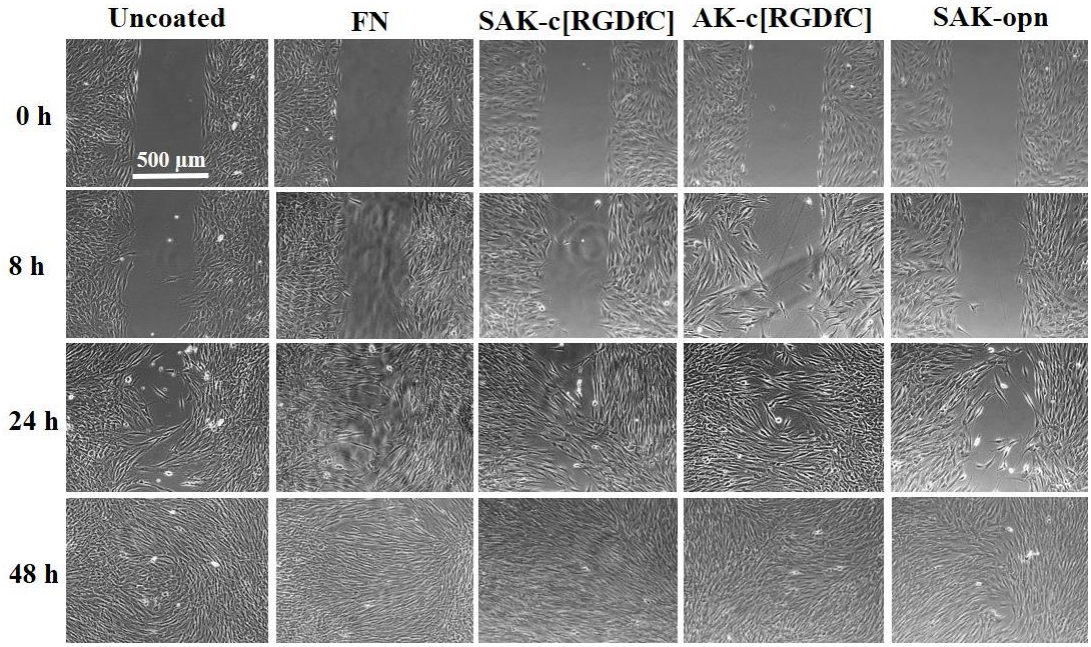


**B)**

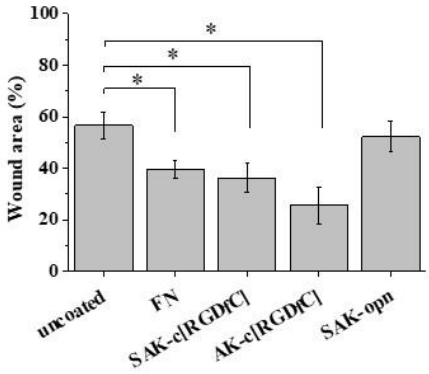


**Figure 6 Cell migration was enhanced on cyclic RGD peptide-coated surfaces**.

**A)** Representative images illustrated wound closure on adhesive coatings. In inverted microscopy, magnification ×100 was used. Scale bar 500 µm. **B)** Wound area after 24 h. Each group was normalized to the wound area measured at 0 h. Data are presented as mean ± standard error (SEM) from 3 independent experiments. Statistical differences compared with uncoated $^{*}p \leq 0.05$.

### 4.1.3 Flow cytometry analysis

Flow cytometry analysis revealed that all PDLSCs expressed CD90, CD73, CD166, integrin α3 (100%); and a high fraction of cells expressed integrin β1 (98.2%) and CD146 (83.3%); a moderate fraction of cells expressed integrin α2 (54.1%), integrin αVβ3 (47.5%), while CD271 (9.3%), CD105 (6.4%), STRO-1 (0.5%) and integrin β7 (0.5%) were detected in a low fraction of PDLSCs (Figure 7).

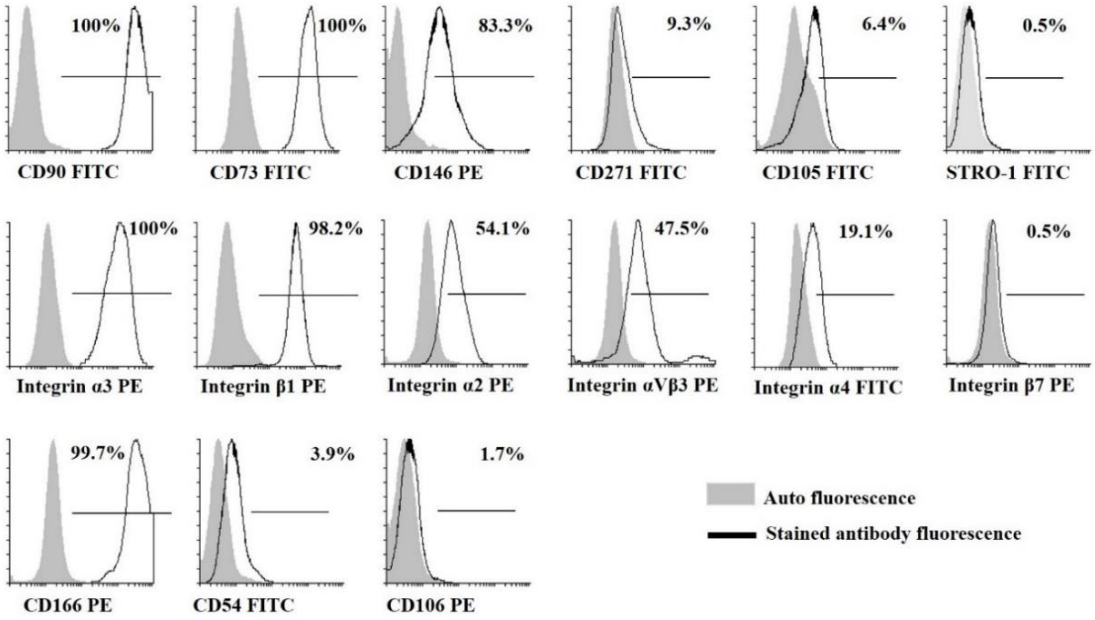


**Figure 7 Flow cytometry characterization of surface markers in PDLSCs.**

Compared with reference cells (HGEP-human gingival epithelial cells and MRC-5 lung fibroblast), the percentage of PDLSCs positive for CD90, CD146, and integrin αVβ3 was higher (Figure 8 A-C); the positive expression % of CD166, integrin β1, and integrin α2 was similarly high (Figure 8 D-E); and the positive expression % of integrin β7, CD54, and CD105 was lower in PDLSCs (Figure 8 G-I) and CD106 was similar low in PDLSCs (Figure 8-J).

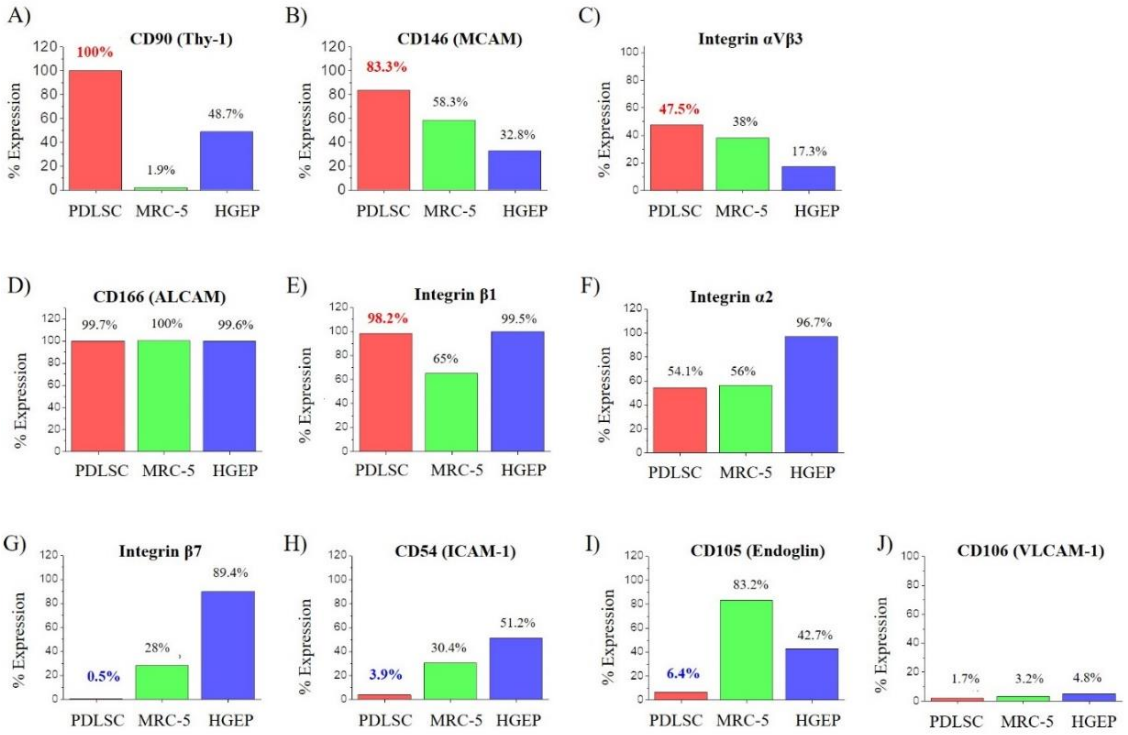


**Figure 8 Percent positivity of cell surface markers in PDLSCs compared to referent cells MRC-5 and HGEP.**

**A)** CD90; **B)** CD146; **C)** integrin αVβ3; **D)** CD166; **E)** integrin β1; **F)** integrin α2; **G)** integirn β7; **H)** CD54; **I)** CD105; and **J)** CD106.

As for treatment with RGD peptides, no major changes were observed in the expression of cell surface molecules in the short-term (1 day); only CD271 positive cell fractions were reduced slightly (0.7 fold). Long-term (1-week) RGD peptide treatments caused an increase in the numbers of PDLSCs positive for MSCs markers; all three RGD peptides increased CD105 (1.7-2.2 fold) and CD146 (1.3-1.5 fold) positive PDLSCs fractions, and CD271 positive cells portion was doubled by AK-c[RGDfC]. Besides, the proportion of PDLSCs positive for cell surface integrins tended to be reduced. AK-c[RGDfC] reduced integrin β1 positive cells portion down to 0.6 fold, SAK-c[RGDfC] and SAK-opn reduced integrin α4 positive cells down to 0.5 fold (Table 1).

**Table 1 Effect of synthetic RGD peptides on the expression of cell surface molecules of PDLSCs.**

After RGD peptide treatments, the mean fluorescence intensity (MFI) of specific antibodies against cell surface molecules was measured with flow cytometry. Changes in the proportion of surface markers positive cells are shown in folds, compared with untreated control.

| | | Fold change in MFI compared with uncoated control | | | | | | | |
|---|---|---|---|---|---|---|---|---|---|
| | | Short-term (1 day) | | | | Long-term (1 week) | | | |
| CD markers | | Uncoated | SAK-c[RGDfC] | AK- c[RGDfC] | SAK-opn | Uncoated | SAK-c[RGDfC] | AK-c[RGDfC] | SAK-opn |
| MSCs markers | CD90 (Thy-1) | 1 | 1.1 | 1.1 | 1.0 | 1 | 1.1 | 1.1 | 1.0 |
| | CD73 | 1 | 0.9 | 0.9 | 0.9 | 1 | **1.4** | 1.2 | 1.1 |
| | CD146 (MCAM) | 1 | 1.1 | 1.0 | 1.1 | 1 | **1.3** | **1.5** | **1.5** |
| | CD271 | 1 | **0.7** | **0.7** | 0.9 | 1 | 1.0 | **2.0** | **1.6** |
| | CD105 (Endoglin) | 1 | 1.1 | 1.2 | 1.1 | 1 | **2.0** | **1.7** | **2.2** |
| | STRO-1 | 1 | 1.0 | 1.0 | 0.9 | 1 | 1.0 | 1.0 | **1.3** |
| Cell adhesion molecules | CD49c (Integrin α3) | 1 | 1.0 | 1.1 | 0.9 | 1 | **1.8** | 1.1 | 1.0 |
| | CD29 (Integrin β1) | 1 | 1.2 | 0.9 | 1.0 | 1 | 0.8 | 0.6 | 0.7 |
| | CD49b (Integrin α2) | 1 | 0.9 | 0.9 | 0.9 | 1 | 1.2 | 1.2 | 1.1 |
| | Integrin αVβ3 | 1 | 0.9 | 0.9 | 1.0 | 1 | 0.9 | 0.8 | 0.9 |
| | CD49d (Integrin α4) | 1 | 0.9 | 1.1 | 1.2 | 1 | 0.5 | 0.9 | 0.5 |
| | Integrin β7 | 1 | 1.0 | 1.0 | 1.1 | 1 | 1.1 | 1.2 | 1.0 |
| | CD166 (ALCAM) | 1 | 1.0 | 0.9 | 1.0 | 1 | 0.9 | 0.8 | 0.8 |
| | CD54 (ICAM-1) | 1 | 1.2 | 1.1 | 0.9 | 1 | 1.1 | 1.0 | 1.3 |
| | CD106 (VCAM-1) | 1 | 0.9 | 1.0 | 1.0 | 1 | **1.4** | 1.0 | 0.7 |

### 4.1.4 Immunofluorescence staining

Immunofluorescence staining for PDLSCs with CD90 and STRO-1 showed a high amount of cells were positively stained with CD90 while very few cells in the population were stained with STRO-1 (Figure 9).

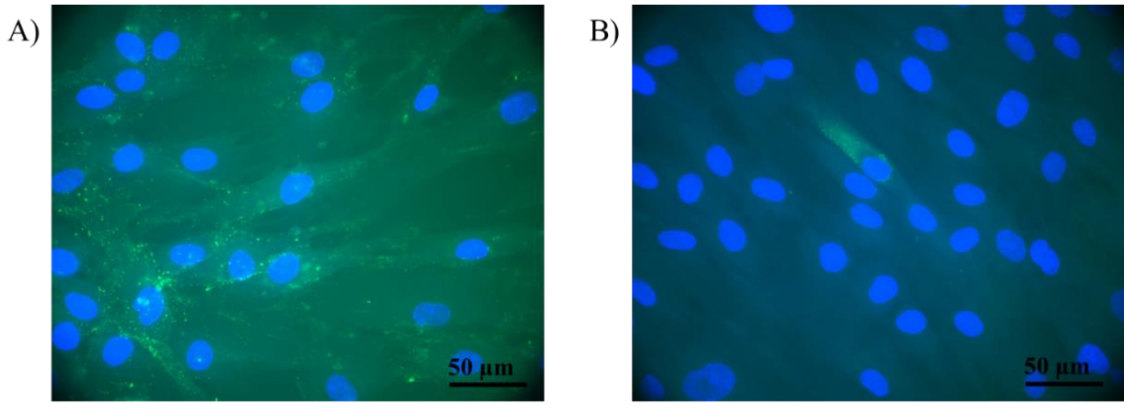


**Figure 9 Immunofluorescence staining images of PDLSCs**.
**A)** CD90 (green) and cell nuclei DAPI (blue); **B)** STRO-1(green) and DAPI (blue). Scale bars 50 µm.

### 4.1.5 Osteogenic differentiation capacity

PDLSCs were seeded on RGD peptide-coated culture ware in a standard culture medium, and after two days when cells are confluent, the medium was replaced with an osteogenic induction medium. In parallel, cells were maintained in a standard medium to identify the effect of synthetic peptides alone without an osteogenic induction medium.

#### 4.1.5.1 ALP activity

After one week, the ALP activity was increased in all osteo-induced groups by more than 4 fold compared to absolute control. Under osteogenic conditions, synthetic peptide-treated cells had all significantly better ALP activity compared with osteo-induced/ uncoated control. In the case of non-induced cultures, the ALP activity was significantly increased in cyclic peptide-treated cells compared to control. After two

weeks, ALP activity in osteo-induced groups was lowered compared with week 1 (Figure 10).

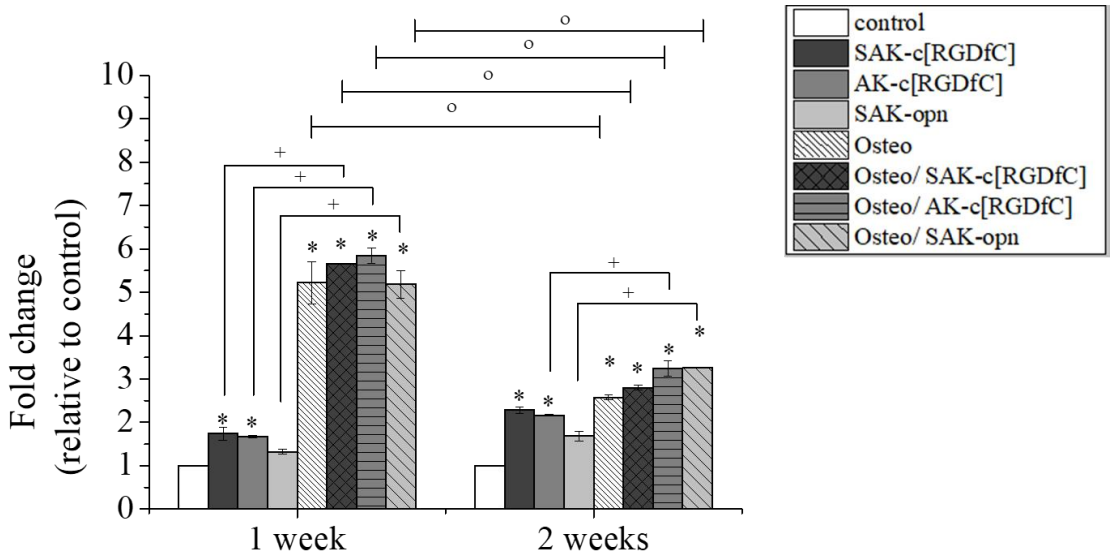


**Figure 10 ALP activity after 1 and 2 weeks of osteogenic induction in PDLSCs.** ALP activity in the experimental groups normalized to the absolute control. Data are presented as mean ± SEM from 3 independent experiments. Statistical differences compared with absolute control *$p \leq 0.05$; peptide treated osteo-induced samples compared to identically treated non-induced $^{+}p \leq 0.05$ and 1-week vs 2-weeks $^{\circ}$ $p \leq 0.05$.

#### 4.1.5.2 Alizarin Red S staining

Alizarin Red S staining was done after three weeks of osteogenic induction to determine calcium deposit. The quantitative value of the staining was obtained as an optical density and evaluated. Strong staining was observed in all osteo-induced cells and mild staining was observed in peptide-treated non-induced cells. In the standard culture, cyclic RGD peptides significantly increased the staining compared with control. Osteo-induced all groups had increased staining compared with absolute control. Compared with osteo-induced uncoated control, the staining was greater in SAK-c[RGDfC], and SAK-opn treated cells. (Figure 11-B, Figure 11-C).

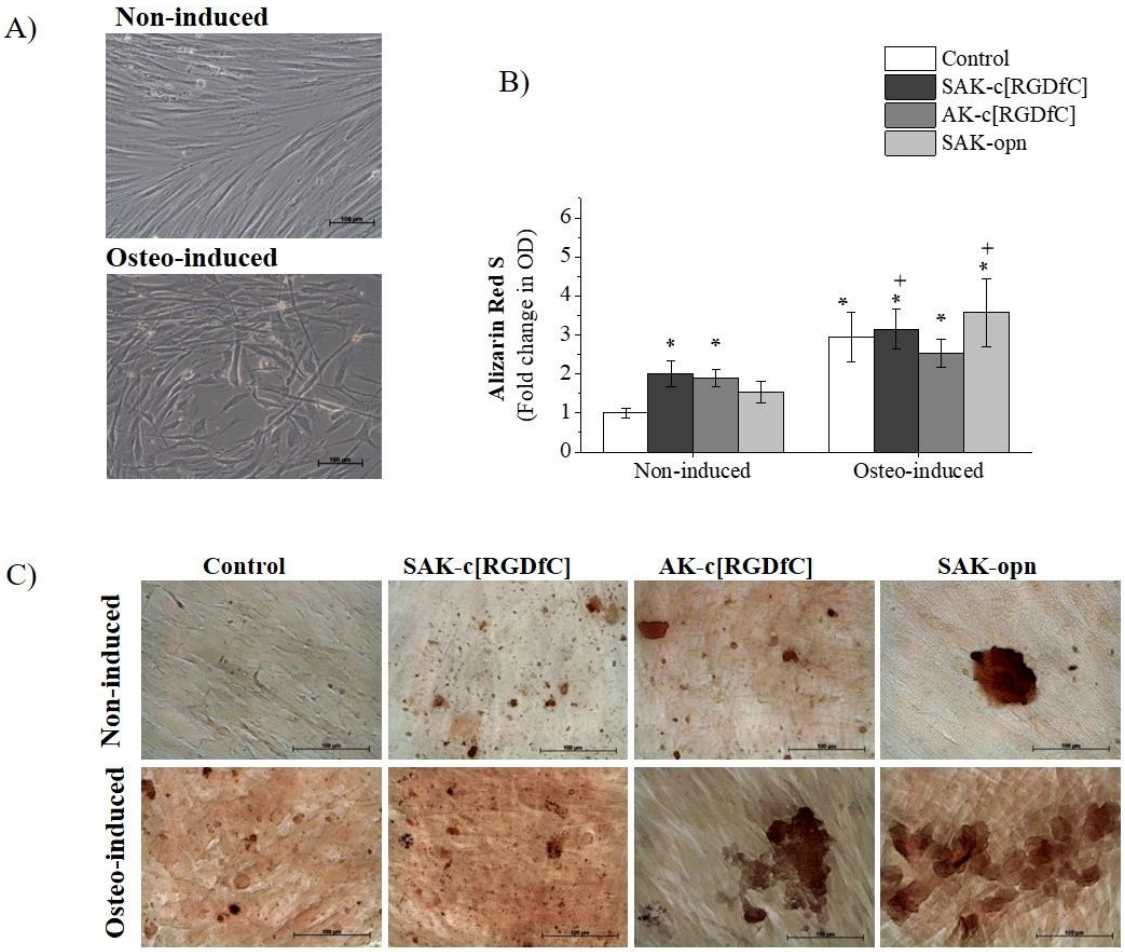


**Figure 11 Osteogenic induction of PDLSCs after 3 weeks.**

Cell morphology was observed: **A)** Inverted microscopy images show cell morphology after three weeks of osteogenic induction of PDLSCs and primary culture of PDLSCs; non-induced cells had long spindle-like morphology, whereas osteo-induced cells appeared shortened and had a more distinguished nucleus. Scale bar 100 µm. **B)** Bar graph shows Alizarin Red S staining normalized to non-induced/ uncoated control. Data are presented as mean ± SEM from 3 independent experiments. Statistical differences compared with absolute control *$p \leq 0.05$ and peptide treated osteo-induced samples compared to identically treated non-induced marked by $^{+}p \leq 0.05$. **C)** Representative microscopic images of Alizarin Red S stained cells. Scale bar 100 µm.

#### 4.1.5.3 Real time-qPCR

To monitor the changes in mRNA levels of the osteogenic marker genes RUNX2, osterix, ALP, and mineralization markers osteocalcin and bone sialoprotein, we performed real-time qPCR assays after two weeks of osteogenic induction (Figure 12).

Preosteoblast marker RUNX showed from 1.3 to 1.5-fold increase in osteo-induced cells, and 1.8 fold in non-induced SAK-opn treated cells respectively, compared with absolute control (Figure 12-A).

The expression of early osteoblast marker osterix was unchanged (Figure 12-B).

The changes in ALPL gene 1.9-2.3 fold in osteo-induced cells and 2.0 fold in non-induced SAK-opn treated cells (Figure 12-C).

Upregulation of osteocalcin was over 2.0 fold in osteo-induced cells, regardless of which peptide was used as surface coating treatment (Figure 12-D).

Compared with absolute control, osteo-induced cells had bone-sialoprotein upregulation 5.0-7.0 fold.

Compared with osteo-induced uncoated, expression of bone-sialoprotein was significantly higher in osteo-induced cells AK-c[RGDfC] coated group, but significantly lower in osteo-induced SAK-opn coated group (Figure 12-E).

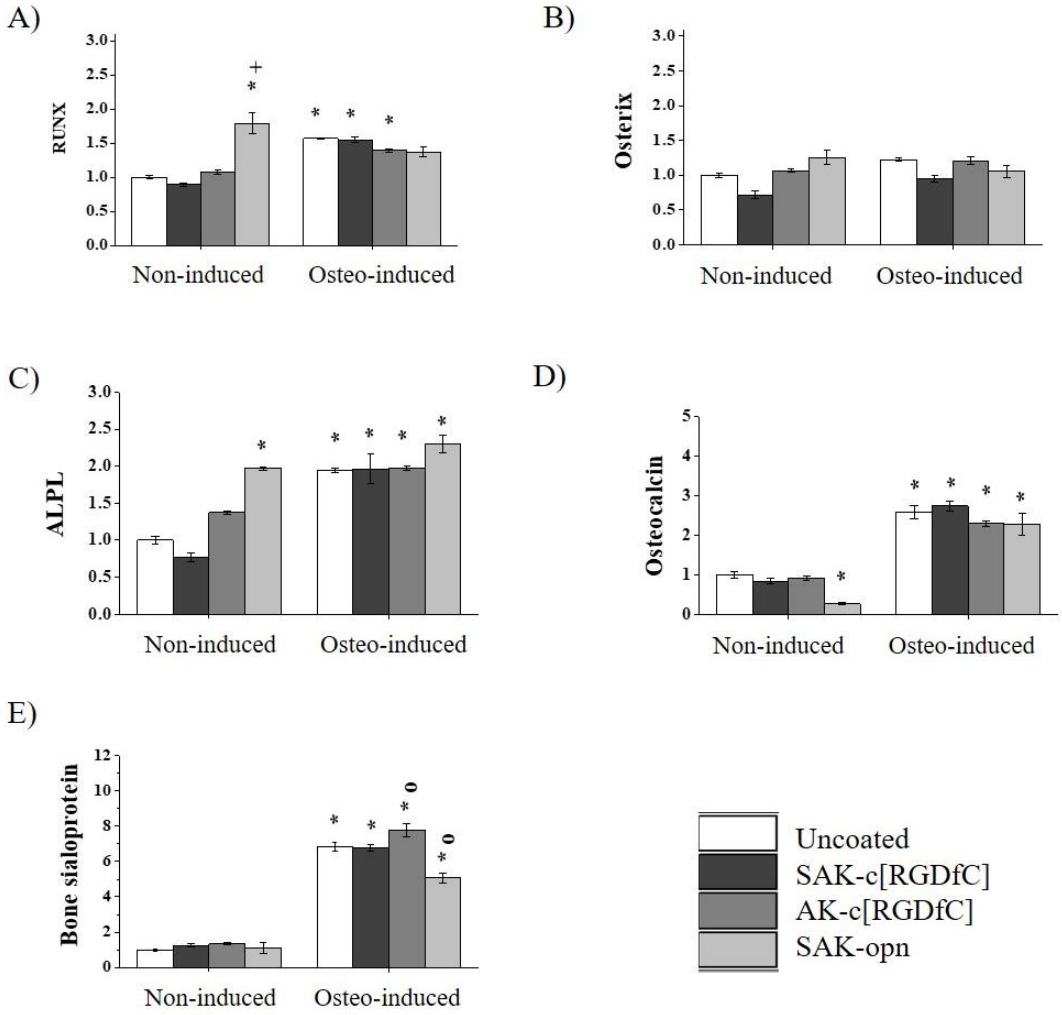


**Figure 12 Real-time qPCR analysis for osteoblast-related genes after two weeks of osteogenic induction**.

Mean expression levels for the target genes are given by RQ values representing relative expression. The expression of each target gene was normalized to that of the RPLP0 housekeeping gene and expressed as fold change relative to absolute control. **A)** RUNX2; **B)** Osterix (SP7); **C)** Alkaline phosphatase (ALPL); **D)** Osteocalcin (BGLAP); and **E)** Bone sialoprotein (IBSP). Statistically significance in experimental groups compared to absolute control $^{*}p \leq 0.05$; peptide treated under osteogenic induction compared to osteo-induced uncoated $^{\circ}p \leq 0.05$; and peptide treated in standard culture compared to identically treated samples in osteo-induced culture $^{+}p \leq 0.05$.

### 4.1.6 Adipogenic differentiation

The ability of PDLSCs to undergo adipogenic differentiation was assessed. During the cultivation with an adipogenic-inductive cocktail, the morphology of PDLSCs changed from spindle-like to squamous-like and wider. Adipogenic induction was held PDLSCs were induced towards adipogenesis (Figure 13-A; Figure 13-B). After three weeks of induction, Oil Red O staining was performed for triglyceride accumulation. Adipo-induced cells had positive oil red O stains surrounding the nucleus. (Figure 13-D) while control cells were not stained (Figure 13-C).

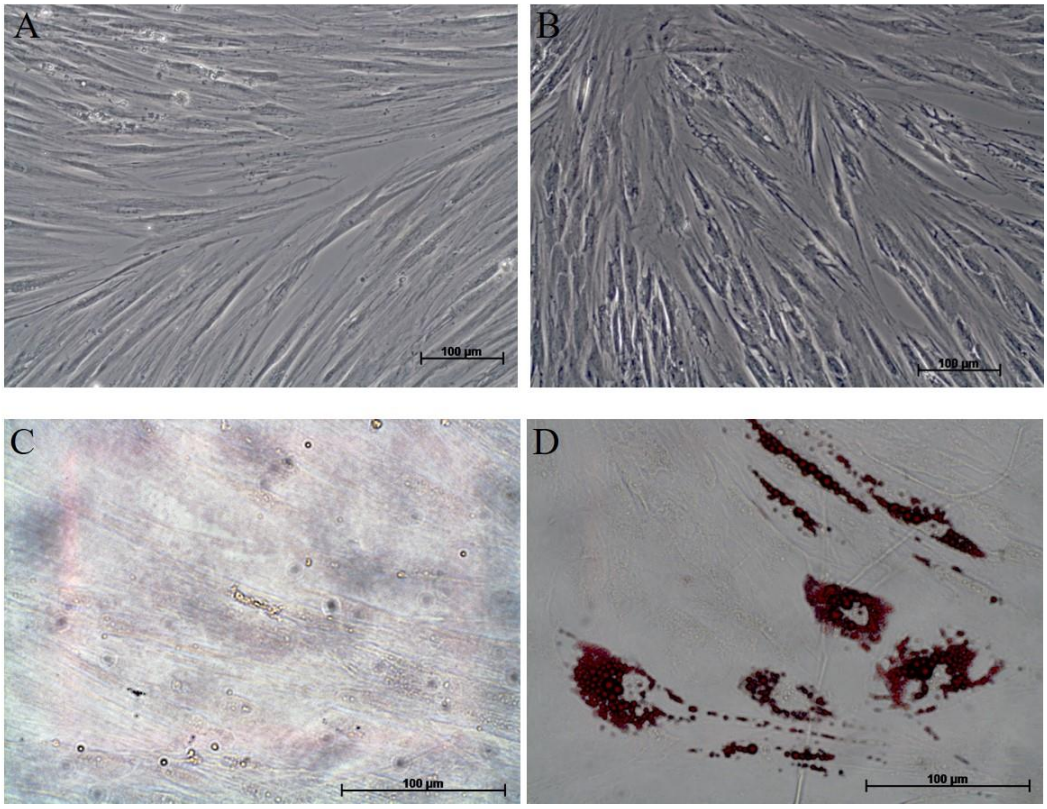


**Figure 13 Adipogenic differentiation of PDLSCs after 3 weeks.**

Cell morphology of PDLSCs: **A)** Non-induced well-attached spindle-shaped cells, **B)** Adipo-induced cells became wider and squamous-like. Oil Red O staining: **C)** control, and **D)** Adipo-induced. Scale bar 100µm.

### 4.1.7 ESIC monitoring for osteogenic and adipogenic differentiation

Osteogenic and adipogenic differentiation of PDLSC was monitored with real-time ECIS non-invasively. Impedimetric arrays were pre-coated with synthetic peptides. Cells were seeded, and ECIS monitoring started. After two days of incubation with a standard medium, osteogenic and adipogenic induction started and was tracked continuously for over 10 days. For data evaluation, complex impedance (Z*) at 64kHz was chosen, as it displayed the most significant differences between experimental groups.

Adipogenic differentiation caused lower impedance compared with control non-induced immediately after the differentiation started. Conversely, osteogenic differentiation presented increased impedance after around 70 h of induction has begun (Figure 14-A).

Regarding peptide treatments, all three experimental peptides elevated impedance during osteogenic differentiation. Also, during adipogenic differentiation, the impedance for cyclic peptides treated groups had significantly increased impedance compared to uncoated adipo-induced control (Figure 14-B).

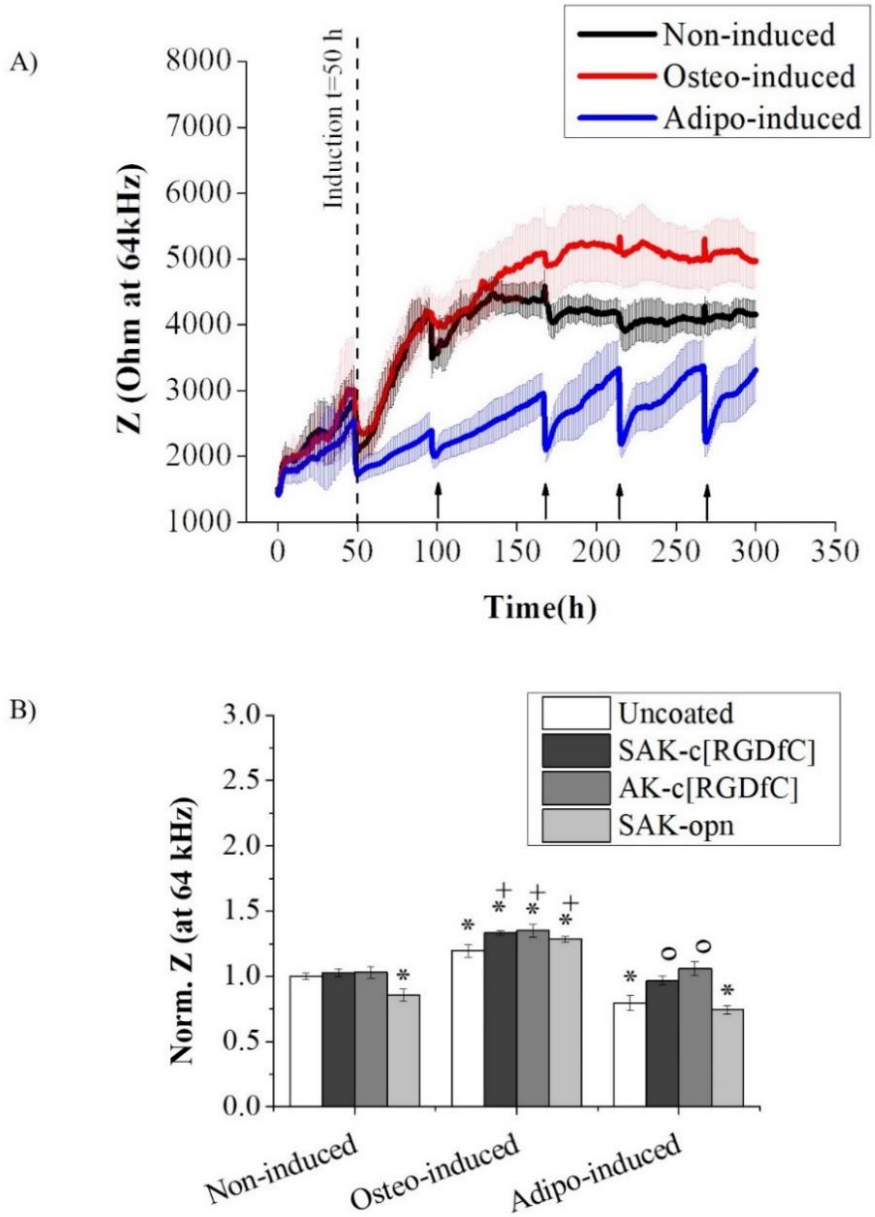


**Figure 14 Cell differentiation was continuously monitored with ECIS for over 10 days.** Osteogenesis and adipogenesis presented different dielectric characteristics. **A)** On the representative graph, complex impedance ($Z^*$) at 64kHz alternating current frequency is plotted against time. Black arrows indicate medium refreshment. **B)** Effect of synthetic peptides on dielectric characteristics of differentiating cells. Post induction 10 days, complex impedance was normalized to uncoated control. Statistically significance in experimental groups compared to absolute control $^*p \leq 0.05$; coated/osteo-induced compared to uncoated/osteo-induced $^+p \leq 0.05$; and coated/ adipo-induced compared to uncoated/ adipo-induced $^\circ p \leq 0.05$.

### 4.2 The effect of anticeptics on the cell viability of PDLSCs

#### 4.2.1 Determination of cell numbers

To detect the appropriate incubation time for alamarBlue®, cell numbers were titrated and incubated with 22 µl reagent for 4 or 6 hours at 37°C, protected from light. As shown in Figure 15-A, the incubation time of 6 hours was suitable to detect PDLSC viability, presenting a linear graph of fluorescence intensity proportional to the cell number.

For determining the optimal concentration for xCELLIgence measurement, the cells were seeded in numbers of $10^3$, $5 \times 10^3$, and $10^4$ per well in E-Plate 96, and CI was recorded for 72 hours (Figure 15-B). The curve graph illustrated the impedance CI of $5 \times 10^3$ and $10^4$ cells/well increased proportionally cell number whereas $10^3$ cells/well did not match this correlation.

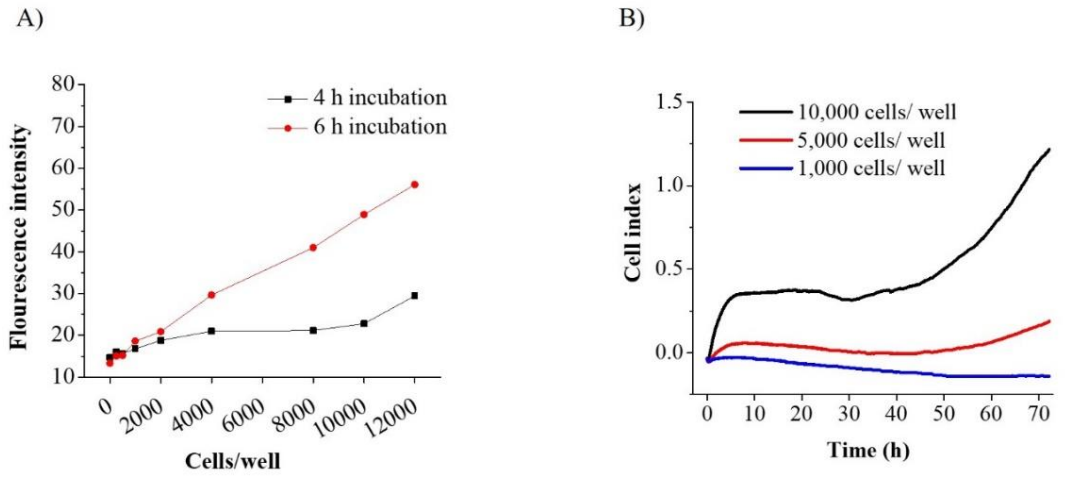


**Figure 15 Plot assay for determination of cell numbers**

**A)** Cell number and resazurin fluorescence correlation linearity checked with Spectrophotometer at 565 and 590 nm wavelengths. **B)** Ideal cell density in 96-well plate was defined with xCELLigence RTCA assay

### 4.2.2 Cell morphology assessment

Cells were treated with antiseptics agents for 24 hours (Figure 16). Untreated control cells showed a long spindle shape and were well-attached to the culture plate.

Exposure to CPC 0.0001 mg/ml did not alter cell morphology or confluence, and CPC 0.001 mg/ml treated cells appeared relatively smaller than control cells in size and some cells were rounded, whereas 0.01 mg/ml and 0.1 mg/ml CPC exposed cells all appeared likely to be detached with a round shape (Figure 16-A).

There were no changes in cell morphology and confluency in CHX 0.001 mg/ml exposed cells compared with control, whereas the majority of cells in CHX 0.01 and 0.1 mg/ml treated groups were detached, and CHX 1 mg/ml caused dense precipitation, and no presence of living cells appeared the wells (Figure 16-B).

Triclosan 0.01 mg/ml did not alter cell morphology and confluency, whereas 0.1 mg/ml lowered cell density and 1 mg/ml had half of the cells in a rounded shape, and 2 mg/ml affected all cells detach (Figure 16-C).

Povidone-iodine 0.1 mg/ml did not alter cell morphology and confluency, whereas 1 mg/ml, 2 mg/ml, and 4 mg/ml lowered cell density and cells appeared thinner than in control (Figure 16-D).

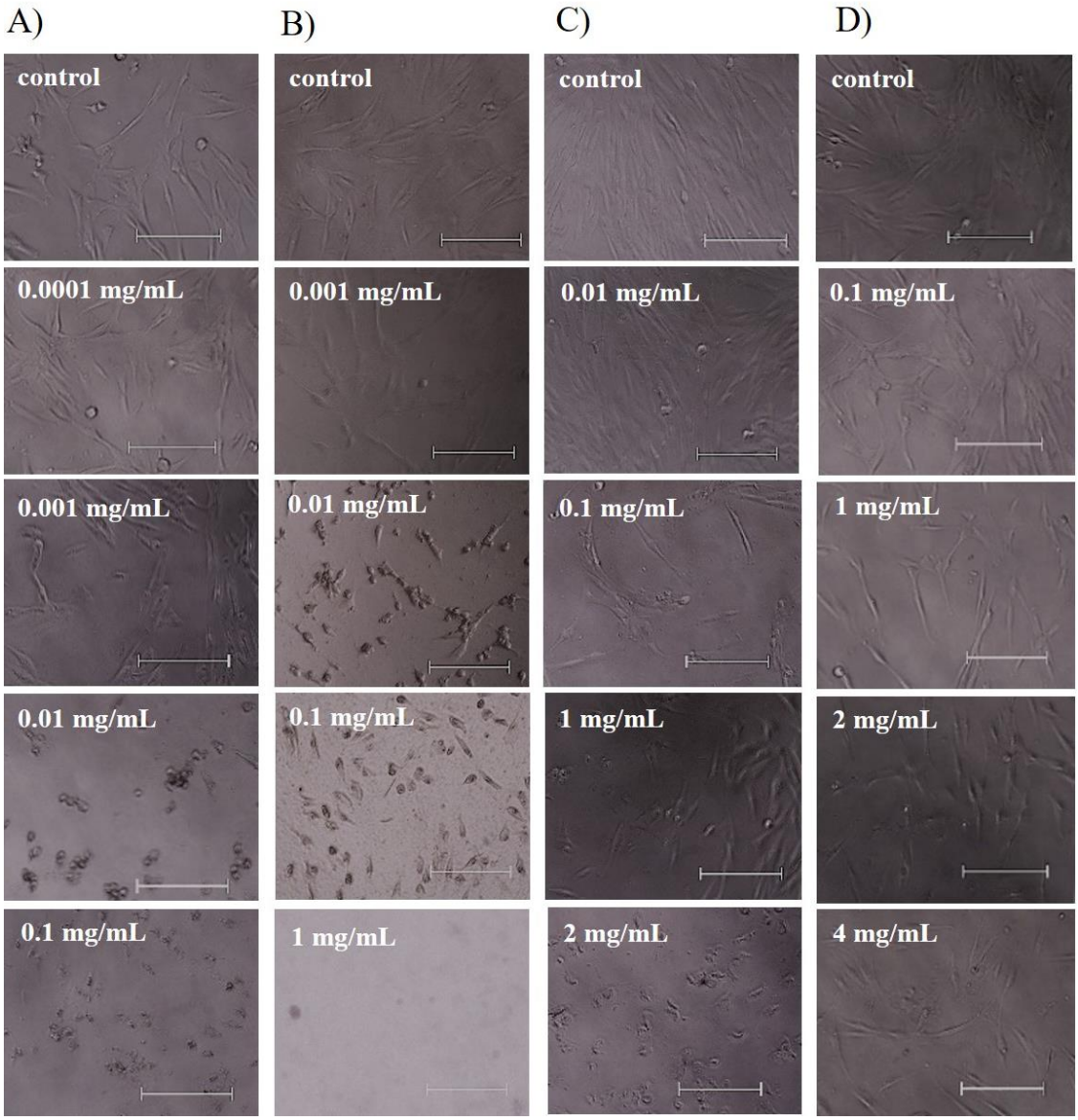


**Figure 16 Cell morphology after 24 h exposure to antiseptic agents.**

Representative images were taken with inverted microscopy. Scale bar 200 µm. **A)** Cetylpiridinium chloride, **B)** Chlorhexidine, **C)** Triclosan, and **D)** Povidone-iodine

### 4.2.3 Cetylpyridinium chloride (CPC)

The alamarBlue® assay results showed cell viability was reduced by CPC 0.1 mg/ml ($p \leq 0.001$), 0.01 mg/ml ($p \leq 0.01$) and 0.001 mg/ml ($p \leq 0.05$) instantly, whereas it was not affected by 0.0001 mg/ml concentration. Long-term exposure to 0.1 mg/ml and 0.01 mg/ml dropped cell viability less than 20% whereas viability of cells those which were exposed to 0.001 mg/ml remained around 80% and 0.0001 mg/ml remained 100% (Figure 17-A).

Impedimetry results indicated CPC 0.1 mg/ml ($p \leq 0.01$) and 0.01 mg ($p \leq 0.01$) reduced cell index instantly in ultra-short-term (Figure 17-B). Long-term monitoring displayed significantly reduced cell index in cells exposed to CPC 0.1 mg/ml 0.01 mg/ml and 0.001 mg/ml (Figure 17-C), the curve slopes 0-12 hours indicated the significance compared with control was $p \leq 0.001$, $p \leq 0.001$, and $p \leq 0.05$ respectively (Figure 17-D). Cell index in 0.0001 mg/ml CPC exposed cells remained indifferent compared with control.

The IC50 value of CPC in PDLSCs after 48-hours contact was according to alamarBlue® assay: 0.002 mg/ml; impedimetry assay: 0.001 mg/ml (Table 2).

### 4.2.4 Chlorhexidine (CHX)

The alamarBlue® assay: ultra-short-term exposure to CHX 1 mg/ml ($p \leq 0.001$) inhibited cell viability in ultra-short-term, and short term exposure to 0.1 mg/ml in dropped it to 30% ($p \leq 0.001$). CHX 0.01 mg/ml did not affect cell viability within 30 minutes, but after 24 hours the cell viability was less than 50% ($p \leq 0.01$), whereas it was slightly increased in 0.001 mg/ml exposed cells ($p \leq 0.05$) (Figure 18-A).

Impedimetry: in ultra-short-term measurement, the cell index was reduced in CHX 1 mg/ml contacted cells ($p \leq 0.01$) while other groups did not show a significant difference (Figure 18-B). After 12 hours of exposure to 1 mg/ml, 0.1 mg/ml, and 0.01 mg/ml, the impedance on the electrode was significantly low compared with control (Figure 18-C; Figure 18-D).

The IC50 value of CHX in PDLSCs after 48 hours of contact was according to alamarBlue® assay: 0.004 mg/ml; impedimetric assay calculated with RTCA software was: 0.0014 mg/ml (Table 2).

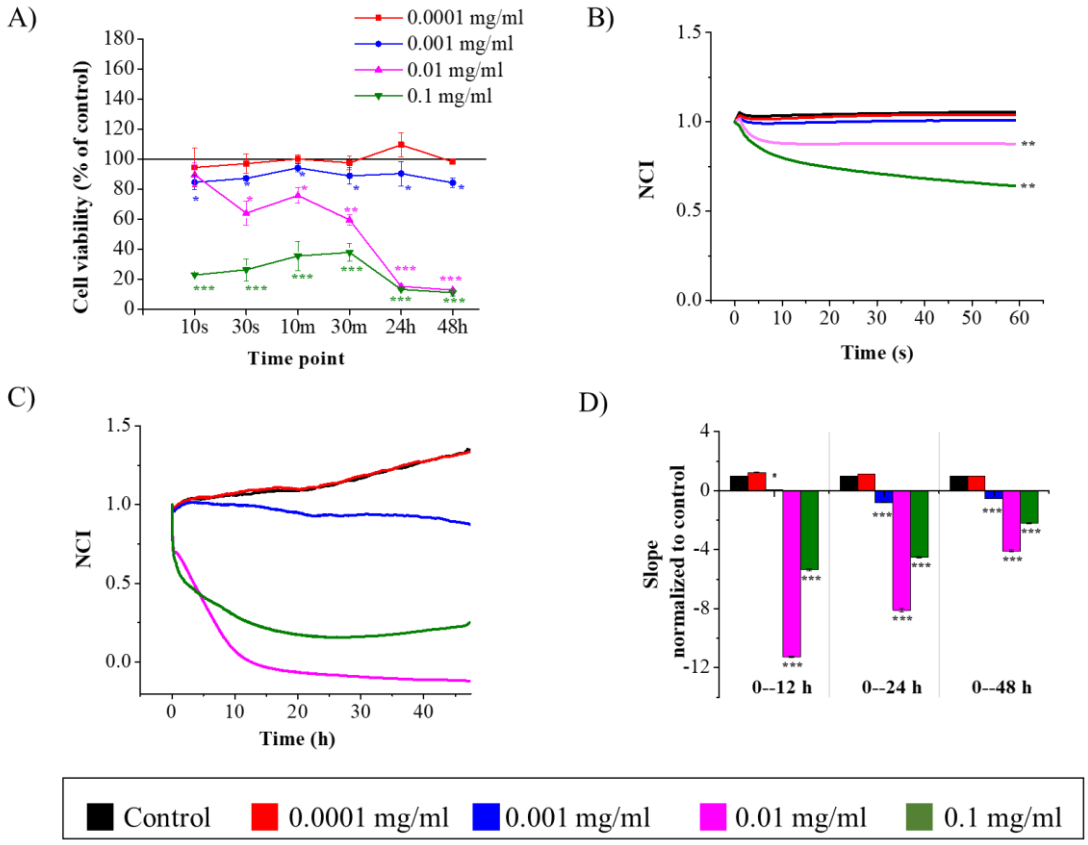


**Figure 17 Viability of PDLSCs during exposure to cetylpyridinium chloride (CPC).** A) alamarBlue® assay results. Measured fluorescence intensity was normalized to control and refers to cell viability (%) at measured time points. The impedimetric analysis results are represented with normalized cell index curve graphs plotted against time in **B)** ultra-short-term (within 1 min duration), **C)** long-term (over 48 h). The normalized slope bar graph (**D)** illustrates dynamics in cell index changes for experimental groups. Statistical differences compared to control; $p^{*} \leq 0.05$; $p^{**} \leq 0.01$; $p^{***} \leq 0.001$

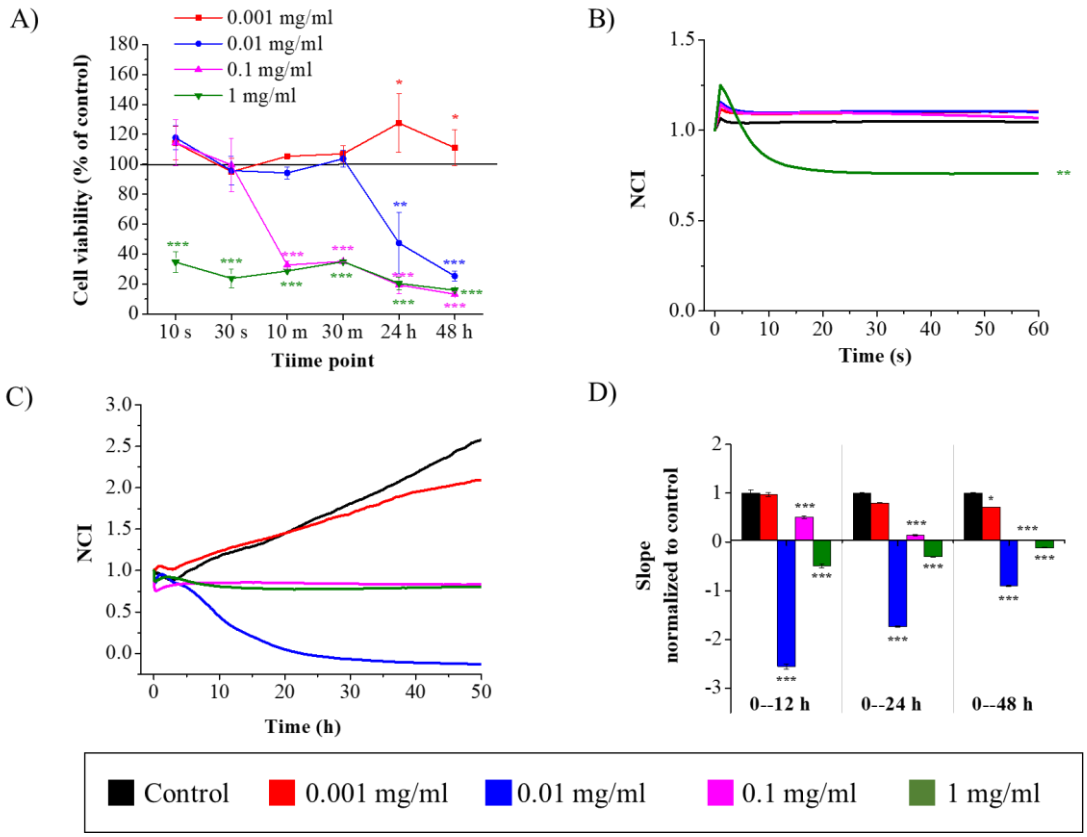


**Figure 18 Viability of PDLSCs during exposure to chlorhexidine (CHX).**

**A)** alamarBlue® assay results. Measured fluorescence intensity was normalized to control and refers to cell viability (%) at measured time points. The impedimetric analysis results are represented with normalized cell index curve graphs plotted against time in **B)** ultra-short-term (within 1 min duration), **C)** long-term (over 48 h). The normalized slope bar graph **(D)** illustrates dynamics in cell index changes for experimental groups. Statistical differences compared to control; $p^{*} \leq 0.05$; $p^{**} \leq 0.01$; $p^{***} \leq 0.001$

### 4.2.5 Triclosan (TCS)

The alamarBlue® assay: TCS 2 mg/ml and 1 mg/ml reduced cell viability down to 60-70% within 30 secs, and it was reducing time-dependently, reaching close to zero by 48 hours. However, exposed to lower concentrations (0.1 mg/ml and 0.01 mg/ml) led to ~10% increase in viability 48 hours (Figure 19-A).

Impedimetry: The electrical impedance was reduced instantly in TCS 2 mg/ml and 1 mg/ml treated cells ($p \leq 0.01$), whereas it was not disturbed with 0.1 mg/ml and 0.01 mg/ml within 1 min duration (Figure 19-B). After 12 hours, cell index for TCS 0.1 mg/ml and 0.01 mg/ml exposed cells were significantly lowered ($p \leq 0.01$); however, the curve appeared to be ascending, whereas higher concentrations led it to close to zero by 48 hours (Figure 19-C; Figure 19-D).

The IC50 value of the TCS calculated from the alamarBlue® assay was TCS 1.25 mg/ml; RTCA analysis was: 0.57 mg/ml (Table 2).

### 4.2.6 Povidone iodine (PVP-I)

alamarBlue® assay: Ultra-short exposure to PVP-I 4 mg/ml ($p \leq 0.001$), 2 mg/ml ($p \leq 0.01$) and 1 mg/ml ($p \leq 0.01$) reduced cell viability. Throughout the measurement time points, viability of cells in contact with 4 mg/ml and 2 mg/ml was downgrading and remained close to zero by the end, the lower concentrations 1 mg/ml and 0.1 mg/ml showed increased fluorescence ($p \leq 0.05$) after 24 hours (Figure 20-A).

Impedimetry: 4 mg/ml, 2 mg/ml and 1 mg/ml significantly decreased cell index in ultra-short-term (Figure 20-B). cell index remained close to zero during long exposures to 4 mg/ml and 2 mg/ml, whereas 1 mg/ml allowed increased impedance signaling after 24 hours which indicated possible growth of survived cells. Povidone-iodine 0.1 mg/ml did not interfere with cell behavior throughout 48 hours of monitoring (Figure 20-C; Figure 20-D)

The IC50 (48 h) value of PVP-I in PDLSCs was according to the alamarBlue® assay 1.4 mg/ml; and according to the RTCA assay, it was 0.7 mg/ml (Table 2).

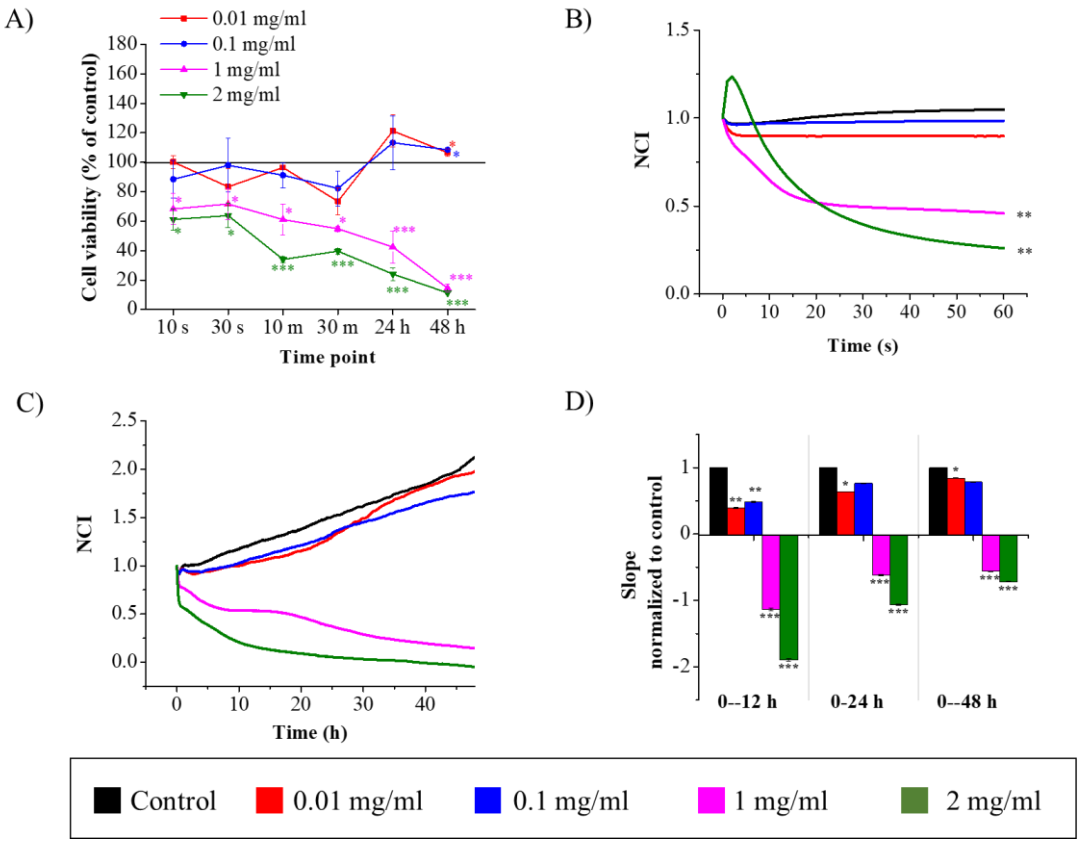


**Figure 19 Viability of PDLCs during exposure to triclosan (TCS).**

**A)** alamarBlue® assay results. Measured fluorescence intensity was normalized to control and refers to cell viability (%) at measured time points. The impedimetric analysis results are represented with normalized cell index curve graphs plotted against time in **B)** ultra-short-term (within 1 min duration), **C)** long-term (over 48 h). The normalized slope bar graph **(D)** illustrates dynamics in cell index changes for experimental groups. Statistical differences compared to control; $p^{*} \leq 0.05$; $p^{**} \leq 0.01$; $p^{***} \leq 0.001$

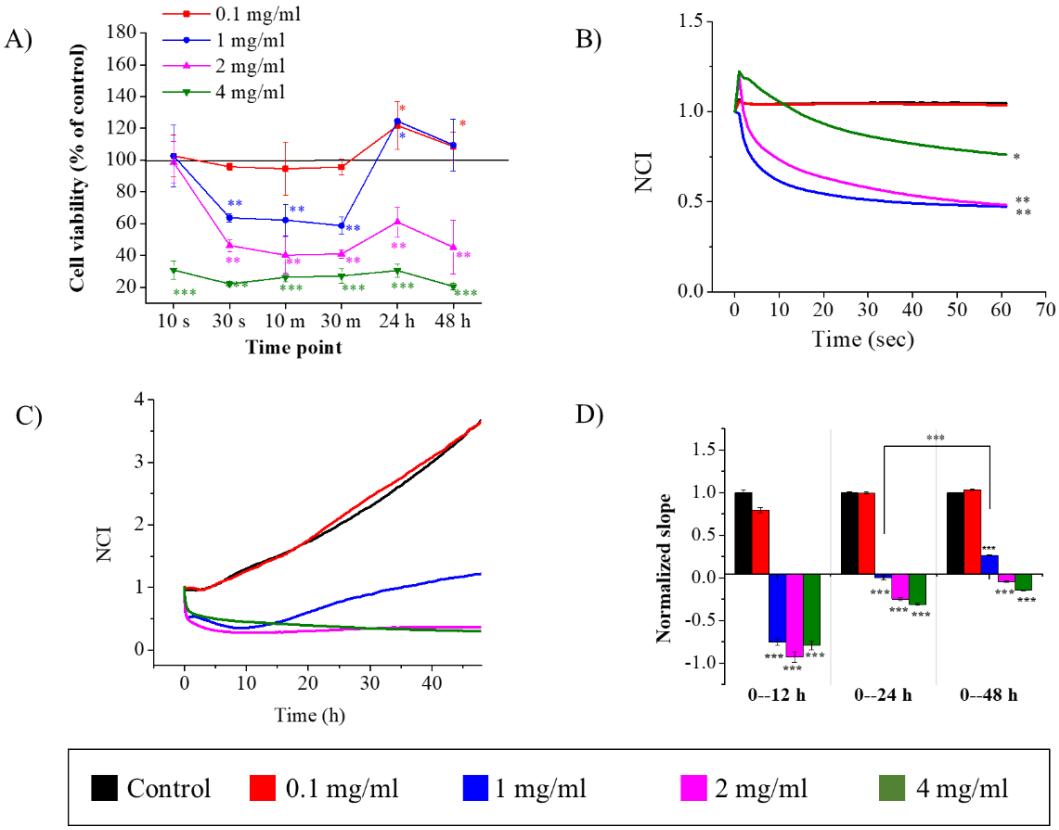


**Figure 20 Viability of PDLSCs during exposure to povidone-iodine (PVP-I)**

**A)** alamarBlue® assay results. Measured fluorescence intensity was normalized to control and refers to cell viability (%) at measured time points. The impedimetric analysis results are represented with normalized cell index curve graphs plotted against time in **B)** ultra-short-term (within 1 min duration), **C)** long-term (over 48 h). The normalized slope bar graph **(D)** illustrates dynamics in cell index changes for experimental groups. Statistical differences compared to control; $p^{*} \leq 0.05$; $p^{**} \leq 0.01$; $p^{***} \leq 0.001$

**Table 2** The half-maximal inhibitory concentration (IC50 value) at 48 h exposure of antiseptic agents to human PDLSCs. Data were represented as mean ±SD, which were obtained from alamarBlue® assay and xCELLigence analysis, each repeated three times (biological replicates) with three technical replicates, respectively.

| | IC50 (mg/ml) at 48 h | |
|---|---|---|
| | alamarBlue® assay | RTCA assay |
| Cetylpyridinium chloride | 0.0022 ± 0.001 | 0.001 ± 0.00008 |
| Chlorhexidine | 0.0037 ± 0.0002 | 0.0014 ± 0.00018 |
| Triclosan | 1.25 ± 0.007 | 0.57 ± 0.3 |
| Povidone-iodine | 1.4 ± 0.17 | 0.7 ± 0.4 |

## 5. DISCUSSION

Periodontal damage is one of the great challenges in current dentistry. Stem cell-based periodontal regenerative therapy is an emerging new method, and periodontal ligament stem cells (PDLSCs) are one of the most suitable candidates. We aimed to establish certain properties of human PDLSCs, including cell functions, cell surface molecules, and cell viability.

Firstly, we evaluated cell adhesion, proliferation, migration, differentiation, and cell surface characteristics of PDLSCs when cultured on synthetic adhesive RGD peptide coatings. Argynyl-glycyl-aspartate (RGD) sequence is an integrin-binding site of ECM proteins. Three different synthetic peptide conjugates were utilized: (i) AK-c[RGDfC]: cyclic RGDfC conjugated to Poly-L-lysin with oligo DL-alanine side branches; (ii) SAK- c[RGDfC]: cyclic RGDfC conjugated to Poly-L-lysin with serine-oligo-DL-alanine branches and (iii) SAK-osteopontin (SAK-opn) osteopontin derived linear Ac-GRGDSVVYGLR-$NH_2$ was conjugated to Poly-L-lysin with serine-oligo-DL-alanine branches.

The animal serum is added to the cell culture medium because it contains various essential factors for cell attachment and spreading. Yet, there are some risks of contamination and possible immune reactions due to its unknown nature if the cells are prepared for clinical application, i.e., human transplantation (123). To avoid these problems, serum-free media are widely used, but most of them impair cell attachment (92). Coating the culture-ware surface with human/animal-derived ECM molecules however support cell attachment, this brings back the risks of contamination and chemically uncertainty. Therefore, chemically defined synthetic materials to enhance cell adhesion and proliferation, an alternative to animal proteins are beneficial for eliminating these risks.

The cell culture ware surfaces were coated with a simple absorbance method with RGD peptides, and for cell adhesion and migration assays, human plasma fibronectin was used as a positive control, and negative control was left uncoated for all assays.

Adhesion and proliferation assays were performed with impedimetric xCELLigence, which is a non-invasive monitoring system to track cell behavior in real-time. The adhesion phase of PDLSCs was completed within 8-10h, and cell proliferation started

after around 40 hours. AK- c[RGDfC] and SAK- c[RGDfC] peptides increased the initial adhesion of PDLSCs either in serum-supplemented or without serum culture environments. Previously, the adhesion inducer effect of AK-c[RGDfC] in serum-free conditions was reported with end-point assays, and it was found that this cyclic peptide promoted initial attachment of fibroblast and BMMSCs when coated on plastic cultureware (92); and SAK-c[RGDfC] conjugate, which has a slightly modified version of backbone molecules, had increased MSCs attachment on titanium surface and bovine bone substitute in serum-free condition (94). Our data suggest that cyclic RGD peptides (AK-c[RGDfC] and SAK-c[RGDfC]) improved cell adhesion likewise fibronectin whether in the presence or absence of animal serum in the culture and all tested synthetic peptides did not harm cell proliferation.

Active migration of progenitor cells towards the injury sites determines regenerative effects and the healing process (124). Cell migration assay results indicated that PDLSCs showed enhanced cell migration on cyclic peptides SAK-c[RGDfC] and AK-c[RGDfC] coated surfaces similarly to fibronectin-coated surfaces, while SAK-opn was ineffective for the cell migration.

Cell surface characterization of PDLSCs was done with flow cytometry analysis. Among checked surface markers, it revealed that >95% of PDLSCs expressed CD90, CD73, CD166, integrin α3, integrin β1; and the majority of PDLSCs expressed CD146 (83%). STRO-1 is one of the major markers of MSC. But STRO-1 has been reported to be expressed in a low number of cells in dental stem cell populations (125). As expected, a very low number of STRO-1 was detected in PDLSCs with flow cytometry and immunofluorescence staining. Compared with human gingival epithelial cells (HGEP) and human lung fibroblast (MRC-5) cells, the percentage of CD90 and CD146 positive cells was much higher in the PDLSCs population. Synthetic RGD peptide treatments affected the proportion of PDLSCs positive for MSC markers. Long-term (1-week) culturing on all three RGD peptide treatments tended to increase CD105 and CD146 positive cells. After one week, the number of PDLSCs positive for integrin α4 and integrin β1 was slightly decreased in RGD peptide-treated cells compared with untreated cells. Integrin αVβ3 was reported to selectively bind to RGD-motif (126), however in our experiments, RGD peptide treated cells showed very little change according to integrin αVβ3 expression. We used the enzymatic cell detachment method

with trypsin and EDTA, and some reports have indicated that trypsin influences the behavior of cell surface molecules (127).

The osteogenic commitment of synthetic RGD peptides on PDLSCs was evaluated. Previous studies have shown that SAK-c[RGDfC] increased matrix mineralization of adipose tissue-derived MSCs when combined with bone substrate materials, titanium implant, and plastic (94). In our study, SAK-c[RGDfC] and AK-c[RGDfC] increased ALP activity and Alizarin Red S staining (calcium level) in standard culture, without any additional osteogenic supplements. Real-time qPCR analysis results presented that two weeks of osteogenic induction in PDLSCs led to upregulation of early osteoblast marker genes RUNX, ALPL; and excessive increase of mature osteoblast markers osteocalcin and bone-sialoprotein. Regarding the RGD peptide treatments, the qPCR results did not reveal significant changes.

ECIS analysis was utilized to examine dynamic cellular processes in adipogenic and osteogenic differentiating cells. The cellular dielectric profile for over 10 days of monitoring has shown that osteogenic differentiation caused a steeper and higher impedance profile, whereas adipogenic differentiation caused a shallower profile. These diverse profiles were similar to the results of those previously described profiles in MSCs according to adipo- and osteogenesis in the previous studies (128-130). The differentiation potential of stem cells is typically evaluated by end-point methods such as staining for distinct markers, proteomic analysis, and gene expression profiling. These methods are time-consuming and invasive for the cells. Our study results suggest ECIS analysis as a reliable method to track down cell differentiation activity for long-term non-invasively.

Antiseptic agents are widely used in dental practice and the chances of direct contact with dental stem cells are high. We aimed to examine whether or not dental antiseptic compounds have significant effects on the viability or morphology of human PDLSCs. The cell viability was analyzed with real-time impedimetric xCELLigence and fluorescence-based alamarBlue® assay (resazurin) under stimuli of antiseptic compounds including chlorhexidine, cetylpyridinium chloride, triclosan, and povidone-iodine for ultra-short (10-30 seconds), short (10-30 minutes), and long term (24-48 hours). To our knowledge, this study is the first report on ultra-short-term impedimetric analysis of the cytotoxic effect of above mentioned antiseptic compounds.

Regarding impedimetric and fluorescence analysis, CPC was the most toxic on PDLSCs. The cytotoxicity of CPC was dose- and time-dependent. Previously, it was reported that 5 minutes of exposure to 1 mg/ml CPC caused disruption in keratinocyte cell layers (131), and commercially available mouthwash solution containing CPC was found to impair osteoblast precursor cell viability (100). Our study showed that less than 1-minute contact with ≥0.01 mg/ml was able to reduce PDLSCs viability, and the long-term presence of ≥ 0.001 mg/ml reduced cell proliferation. According to our results, the half-maximal inhibitory concentration (IC50) for CPC on PDLSCs was ≥ 0.002 mg/ml, which was much less than the practically recommended concentration for CPC (0.45-0.7 mg/ml).

Cytotoxicity of CHX was previously verified on a variety of cells such as human fibroblast (132),(133), (134); myoblast (135), osteoblast (136), mouse osteoblast precursor cells (100), odontoblast-like cells (137) and stem cells exfoliated deciduous teeth (101). Cline et al. (138) reported direct exposure to ≥0.025 mg/ml suppressed PDLSCs growth by about 90%; Chang et al. (139) indicated that chlorhexidine ≥0.001 mg/ml was cytotoxic to human PDLSCs. In our observation, CHX 1 mg/ml and 0.1 mg/ml concentrations instantly inhibited PDLSCs viability. Microscopic observation revealed that high concentrations of CHX (1 mg/ml and 0.1 mg/ml) caused dense precipitation. Therefore, during the impedimetry analysis, cell index curves for CHX 1 mg/ml and 0.1 mg/ml concentrations failed to show any dynamics. This can be explained that in the animal serum-supplemented culture medium CHX caused immediate precipitation (140), and it acted as an insulator on the electrode surface. xCELLigence results showed that CHX in lower concentrations 0.01 mg/ml and 0.001 mg/ml, decreased cell viability in long-term. However, resazurin assay result showed that 0.001 mg/ml did not hinder cell viability, rather increased it. Use of the CHX in dental practice is considered as a “gold standard’ and wide range of concentrations from 1 mg/ml to 50 mg/ml are recommended depending on type of products and treatment. Our results showed the IC50 value of CHX was 0.001-0.003 mg/ml (at 48 h) on PDLSCs.

Because of potential health concerns, for instance, antimicrobial resistance and endocrine disruption, and concerning environmental effects, TCS has been banned in some countries (113); however, in dental products, the use of TCS is continued as it is

an effective anti-plaque and antibacterial material (141), (142). Previous studies revealed TCS was cytotoxic to neural stem cells in a dose- and time-dependent manner, and 50 μM (equal to 0.015 mg/ml) or higher concentrations minimum of 3 h was capable of decreasing cell viability (143). Our results on PDLSCs presented TCS ≥ 1 mg/ml concentration was able to decrease cell viability within a minute and suppress proliferation in the long term. The IC50 value at 48 h ranged between 0.6-1.3 mg/ml on PDLSCs.

Resazurin staining and impedimetry results were complementary on 1 mg/ml, or higher concentrations of PVP-I were able to decrease cell viability within 1 min exposure, subsequently (24-48 h); and 1 mg/ml added culture showed signs of survived cells. These were approximate to previous study results; 10-seconds of contact with PVP-I ≥0.77 mg/ml decreased viability of osteoblast cells and impaired differentiation; however, surviving cells showed good recovery and mineralization potential (144). In dental practice, 0.5– 10 mg/ml PVP-I has been applied. In our study, the IC50 concentration (48 h) of PVP-I was 0.7 -1.4 mg/ml on PDLSCs.

One of the limitations of our cell viability assays is that *in-vitro* cell culture does not clearly represent a surgical periodontal wound in vivo. The conditions in the periodontal wound, including vascularization, different cell types, inflammatory responses are not present in monolayer culture, and therefore further study to investigate the effect of dental antiseptics on periodontal tissue healing and tissue regeneration *in-vivo* is necessary.

Taken together, our results showed that PDLSCs adhesion, migration, and osteogenic differentiation were improved with cyclic RGD peptide coatings; and commonly used dental antiseptic agents cetylpyridinium chloride and chlorhexidine were highly toxic to the PDLSCs.

## 6. CONCLUSIONS

Human PDLSCs presented some MSCs cell surface molecules and successfully differentiated towards osteogenic and adipogenic lineages. The differentiation capacity of PDL-derived cells towards osteogenic and adipogenic lineages was documented with conventional end-point assays as well as non-invasive impedimetric analyses.

Adhesion of PDLSCs was promoted when cultivated on SAK-c[RGDfC] and AK-c[RGDfC] peptide coatings, and migration was enhanced compared to that of fibronectin. In the absence of serum in the culture medium, these cyclic RGD peptides increased cell adhesion, and cells remained firmly attached to the cyclic peptide-coated surfaces throughout three days of monitoring. Moreover, synthetic RGD peptides increased matrix mineralization in PDLSCs. Together with this and previous study outcomes suggest that these cyclic peptide conjugates are the potential for application for artificial cell substrates to promote cell adhesion and cell attraction.

Antiseptic agents exerted a cytotoxic effect on PDLSCs in a dose-dependent manner and reduced cell viability and proliferation at lower than practically used concentrations. Among tested compounds, CPC and CHX were highly cytotoxic; PVP-I and TCS were moderately toxic in PDLSCs *in vitro* culture.

Impedimetric xCELLigence monitoring proved to be a non-invasive and time-saving method to determine cell viability.

## 7. SUMMARY

This Ph.D. research project was done in two parts:

In the first part, PDL-derived stem cells (PDLSCs) functions including adhesion, proliferation, migration, differentiation potential, and cell surface characteristics were evaluated on integrin-binding RGD sequence containing synthetic polypeptide coatings. The PDLSCs expressed MSCs surface markers and were capable of differentiating into osteogenic and adipogenic lineages. We found that cyclic RGD containing conjugates SAK-c[RGDfC] and AK-c[RGDfC] promoted cell adhesion, migration, and increased matrix mineralization in PDLSCs. These cyclic RGD conjugates are approved to be applicable biomimetic materials for artificial surface modification with the purpose of cell attracting, particularly for mineralized tissue repairing such as bone regeneration.

In the second part of this work, the viability of cultivated PDLSCs was assessed when exposed to dental antiseptic compounds. Dental antiseptic compounds cetylpyridinium chloride and chlorhexidine were highly toxic, whereas triclosan and povidone-iodine were moderately toxic to PDLSCs. Less than 1-minute contact with these compounds at lower than practically recommended concentrations all immediately decreased cell viability. These findings suggest a cautious use of antiseptic agents when there is possible exposure to an open periodontal wound or during stem cell-based regenerative therapies.

These findings suggest a cautious use of antiseptic agents when there is possible exposure to an open periodontal wound or during stem cell-based regenerative therapies.

## 8. ÖSSZEFOGLALÁS

A Ph.D. kutatási munka két részből áll:

Az első részben a PDL-eredetű őssejtek (PDLSC-k) funkcióit, köztük az adhéziót, proliferációt, migrációt, differenciálódási potenciált, valamint a sejtfelszíni jellemzőket vizsgáltuk szintetikus polipeptid bevonatokat tartalmazó integrinkötő RGD szekvenciákon.

A PDLSC-k expresszáltak MSC felszíni markereket és képesek voltak oszteogén és adipogén vonalakká differenciálódni. Megfigyeltük, hogy a ciklikus RGD-t tartalmazó SAK-c[RGDfC] és AK-c[RGDfC] konjugátumok elősegítették a sejtadhéziót, a migrációt és a PDLSC-kben a mátrix mineralizációjának fokozódását. A vizsgálataink szerint ezek a ciklikus RGD konjugátumok használhatók biomimetikus anyagként mesterséges felületmódosításhoz sejtvonzás céljából, különösen mineralizált szövetek helyreállításánál, például csontregenerációban.

A munka második részében megvizsgáltuk a fogászati antiszeptikus vegyületek PDLSC sejttenyészetek életképességére gyakorolt hatását. A fogászati antiszeptikus vegyületek közül a cetil-piridinium-klorid és a klórhexidin erősen, míg a triklozán és a povidon-jód mérsékelten volt mérgező a PDLSC-kre. Ezt a hatást már egy percnél rövidebb ideig történő érintkezés esetén is, a sejtek életképessége azonnal csökkent, még a klinikai gyakorlatban javasoltnál alacsonyabb koncentráció alkalmazása esetén is tapasztaltuk. Az eredmények ismeretében az antiszeptikus szerek javasolt óvatosan használni nyílt parodontális sebek esetén vagy őssejt-alapú regeneratív terápia során.

## 9. REFERENCES


1. Scannapieco FA, Gershovich E. (2020). The prevention of periodontal disease—An overview. Periodontol 2000, 84(1):9–13.

2. Liccardo D, Cannavo A, Spagnuolo G et nrico, Ferrara N, Cittadini A, Rengo C, Rengo G. (2019). Periodontal disease: A risk factor for diabetes and cardiovascular disease. Int J Mol Sci, 20(6).

3. Zanella SM, Pereira SS, Barbisan JN, Vieira L, Saba-Chujfi E, Haas AN, and Rösing CK. (2016). Periodontal disease, tooth loss and coronary heart disease assessed by coronary angiography: a cross-sectional observational study. J Periodontal Res. 51(2):221–7.

4. Tonsekar PP, Jiang SS, Yue G. (2017). Periodontal disease, tooth loss and dementia: Is there a link? A systematic review. Gerodontology, 34(2):151–63.

5. Michaud DS, Fu Z, Shi J, Chung M. (2017). Periodontal disease, tooth loss, and cancer risk. Epidemiol Rev, 39(1):49–58.

6. Mao AS, Mooney DJ. (2015). Regenerative medicine: Current therapies and future directions. Proc Natl Acad Sci U S A, 112(47):14452–9.

7. Mark Bartold P, G Mcculloch CA, Sampath Narayanan A, Pitaru S. (2000). Tissue engineering: a new paradigm for periodontal regeneration based on molecular and cell biology. Periodontology, 24:253–69.

8. Bartold PM, Gronthos S, Ivanovski S, Fisher A, Hutmacher DW. (2016). Tissue engineered periodontal products. J Periodontal Res, 51(1):1-15.9.

10. Villar CC, Cochran DL. (2010). Regeneration of periodontal tissues: guided tissue regeneration. Dent Clin North Am, 54(1):73-92.

11. Kao RT, Nares S, Reynolds MA. (2015). Periodontal regeneration - intrabony defects: a systematic review from the AAP Regeneration Workshop. J Periodontol, 86(2 Suppl):S77-104.

12. Lin Z, Rios HF, Cochran DL.(2015). Emerging Regenerative Approaches for

Periodontal Reconstruction: A Systematic Review From the AAP Regeneration Workshop. J Periodontol, 86(2-s):S134–52.

13. Nuñez J, Vignoletti F, Caffesse RG, Sanz M. (2019). Cellular therapy in periodontal regeneration. Periodontol 2000, 79(1):107–16.

14. Lang H, Schiiler N, Arnhold S, Nolden R, Mertens T. (1995). Formation of Differentiated Tissues in vivo by Periodontal Cell Populations Cultured in vitro. J Dent Res, 74(5):1219–25.

15. Kolios G, Moodley Y. (2013). Introduction to stem cells and regenerative medicine. Respiration, 85(1):3–10.

16. Ennis WJ, Sui A, Bartholomew A. (2013). Stem Cells and Healing: Impact on Inflammation. Adv Wound Care, 2(7):369–78.

17. Morrison SJ, Spradling AC. (2008). Stem cells and niches: mechanisms that promote stem cell maintenance throughout life. Cell, 132(4):598–611.

18. Thomson JA, Itskovitz-Eldor J, Shapiro SS, Waknitz MA, Swiergiel JJ, Marshall VS, Jones JM. (1998). Embryonic stem cell lines derived from human blastocysts. Science, 282(5391):1145–7.

19. Volarevic V, Markovic BS, Gazdic M, Volarevic A, Jovicic N, Arsenijevic N, Armstrong L, Djonov V, Lako M, Stojkovic M. (2018). Ethical and Safety Issues of Stem Cell-Based Therapy. Int J Med Sci, 15(1):36–45.

20. Weissman IL. (2000). Stem cells: units of development, units of regeneration, and units in evolution. Cell, 100(1):157–68.

21. Suman S, Domingues A, Ratajczak J, Ratajczak MZ. (2019). Potential Clinical Applications of Stem Cells in Regenerative Medicine. Adv Exp Med Biol, 1201:1-22.

22. Lin NH, Gronthos S, Bartold PM. (2008). Stem cells and periodontal regeneration. Aust Dent J, 53(2):108–21.

23. Rajabzadeh N, Fathi E, Farahzadi R. (2019). Stem cell-based regenerative medicine. Stem Cell Investig, 18;6:19.

24. Miletich I, Sharpe PT. (2004). Neural crest contribution to mammalian tooth formation. Birth Defects Res Part C - Embryo Today Rev, 72(2):200–12.

25. Egusa H, Sonoyama W, Nishimura M, Atsuta I, Akiyama K. (2012). Stem cells in dentistry--part I: stem cell sources. J Prosthodont Res, 56(3):151-65.

26. Gan L, Liu Y, Cui D, Pan Y, Zheng L, Wan M. (2020). Dental Tissue-Derived Human Mesenchymal Stem Cells and Their Potential in Therapeutic Application. Stem Cells Int, 1;2020:8864572.

27. Gronthos S, Mankani M, Brahim J, Robey PG, Shi S. (2000). Postnatal human dental pulp stem cells (DPSCs) in vitro and in vivo. Proc Natl Acad Sci U S A, 5;97(25):13625-30.

28. Gronthos S, Brahim J, Li W, Fisher LW, Cherman N, Boyde A, DenBesten P, Robey PG, Shi S. (2002). Stem cell properties of human dental pulp stem cells. J Dent Res, 81(8):531-5.

29. Miura M, Gronthos S, Zhao M, Lu B, Fisher LW, Robey PG, Shi S. (2003). SHED: stem cells from human exfoliated deciduous teeth. Proc Natl Acad Sci U S A, 13;100(10):5807-12.

30. Seo BM, Miura M, Gronthos S, Bartold PM, Batouli S, Brahim J, Young M, Robey PG, Wang CY, Shi S. (2004). Investigation of multipotent postnatal stem cells from human periodontal ligament. Lancet, 364(9429):149-55.

31. Sonoyama W, Liu Y, Fang D, Yamaza T, Seo BM, Zhang C, Liu H, Gronthos S, Wang CY, Wang S, Shi S. (2006). Mesenchymal stem cell-mediated functional tooth regeneration in swine. PLoS One, 20;1(1):e79.

32. Morsczeck C, Götz W, Schierholz J, Zeilhofer F, Kühn U, Möhl C, Sippel C, Hoffmann KH. (2005). Isolation of precursor cells (PCs) from human dental follicle of wisdom teeth. Matrix Biol, 24(2):155-65.

33. Beertsen W, Mcculloch CAG, Sodek J. (1997) The periodontal ligament: A unique, multifunctional connective tissue. Periodontol 2000, 13(1):20–40.

34. Gay IC, Chen S, MacDougall M. (2007). Isolation and characterization of

multipotent human periodontal ligament stem cells. Orthod Craniofac Res, 10(3):149–60.

35. Zhu W, Liang M. (2015). Periodontal ligament stem cells: current status, concerns, and future prospects. Stem Cells Int, 2015:972313.

36. Hu L, Liu Y, Wang S. (2018). Stem cell-based tooth and periodontal regeneration. Oral Dis, 24(5):696-705.

37. Eleuterio E, Trubiani O, Sulpizio M, Di Giuseppe F, Pierdomenico L, Marchisio M, Giancola R, Giammaria G, Miscia S, Caputi S, Di Ilio C, Angelucci S. (2013). Proteome of human stem cells from periodontal ligament and dental pulp. PLoS One, 8(8):e71101.

38. Shi S, Bartold PM, Miura M, Seo BM, Robey PG, Gronthos S. (2005). The efficacy of mesenchymal stem cells to regenerate and repair dental structures. Orthod Craniofac Res, 8(3):191–9.

39. Liu J, Li Q, Liu S, Gao J, Qin W, Song Y, Jin Z. (2017). Periodontal Ligament Stem Cells in the Periodontitis Microenvironment Are Sensitive to Static Mechanical Strain. Stem Cells Int, 2017:1380851.

40. Tomokiyo A, Wada N, Maeda H. (2019). Periodontal Ligament Stem Cells: Regenerative Potency in Periodontium. Stem Cells Dev, 28(15):974–85.

41. Kadar K, Kiraly M, Porcsalmy B, Molnar B, Racz GZ, Blazsek J, Kallo K, Szabo EL, Gera I, Gerber G, Varga G. (2009). Differentiation potential of stem cells from human dental origin - promise for tissue engineering. J Physiol Pharmacol, 60 Suppl 7:167-75.

42. Földes A, Kádár K, Kerémi B, Zsembery Á, Gyires K, S Zádori Z, Varga G. (2016). Mesenchymal Stem Cells of Dental Origin-Their Potential for Antiinflammatory and Regenerative Actions in Brain and Gut Damage. Curr Neuropharmacol, 14(8):914-934.

43. Liu O, Xu J, Ding G, Liu D, Fan Z, Zhang C, Chen W, Ding Y, Tang Z WS. (2013). Periodontal ligament stem cells regulate B lymphocyte function via programmed cell death protein 1. Stem Cells, 31(7):1371–82.

44. Ding G, Liu Y, Wang W, Wei F, Liu D, Fan Z, An Y, Zhang C, Wang S. (2010). Allogeneic periodontal ligament stem cell therapy for periodontitis in swine. Stem Cells, 28(10):1829-38.

45. Tomokiyo A, Wada N, Hamano S, Hasegawa H, Sugii H, Yoshida S, Maeda H. (2016). Periodontal ligament stem cells in regenerative dentistry for periodontal tissues. J Stem Cell Res Ther, 1(3):100-102.

46. Kaku M, Komatsu Y, Mochida Y, Yamauchi M, Mishina Y, Ko C-C. (2012). Identification and characterization of neural crest-derived cells in adult periodontal ligament of mice. Arch Oral Biol, 57(12):1668–75.

47. Huang C-YC, Pelaez D, Dominguez-Bendala J, Garcia-Godoy F, Cheung HS. (2009). Plasticity of stem cells derived from adult periodontal ligament. Regen Med, 4(6):809–21.

48. Alvarez R, Lee HL, Wang CY, Hong C. (2015). Characterization of the osteogenic potential of mesenchymal stem cells from human periodontal ligament based on cell surface markers. Int J Oral Sci, 18;7(4):213-9.

49. Trubiani O, Zalzal SF, Paganelli R, Marchisio M, Giancola R, Pizzicannella J, Bühring HJ, Piattelli M, Caputi S, Nanci A. (2010). Expression profile of the embryonic markers nanog, OCT-4, SSEA-1, SSEA-4, and frizzled-9 receptor in human periodontal ligament mesenchymal stem cells. J Cell Physiol, 225(1):123-31.

50. Iwasaki K, Komaki M, Yokoyama N, Tanaka Y, Taki A, Kimura Y, Takeda M, Oda S, Izumi Y, Morita I. (2013). Periodontal ligament stem cells possess the characteristics of pericytes. J Periodontol, 84(10):1425-33.

51. Tsumanuma Y, Iwata T, Washio K, Yoshida T, Yamada A, Takagi R, Ohno T, Lin K, Yamato M, Ishikawa I, Okano T, Izumi Y. (2011). Comparison of different tissue-derived stem cell sheets for periodontal regeneration in a canine 1-wall defect model. Biomaterials, 32(25):5819-25.

52. van Dijk LJ, Schakenraad JM, van der Voort HM, Herkströter FM, Busscher HJ. (1991). Cell-seeding of periodontal ligament fibroblasts. A novel technique to

create new attachment. A pilot study. J Clin Periodontol, 18(3):196–9.

53. Lang H, Schüler N, Nolden R. (1998). Attachment formation following replantation of cultured cells into periodontal defects--a study in minipigs. J Dent Res, 77(2):393–405.

54. Malekzadeh R, Hollinger JO, Buck D, Adams DF, McAllister BS. (1998). Isolation of human osteoblast-like cells and in vitro amplification for tissue engineering. J Periodontol, 69(11):1256–62.

55. Bright R, Hynes K, Gronthos S, Bartold PM. (2015). Periodontal ligament-derived cells for periodontal regeneration in animal models: A systematic review. J Periodontal Res, 50(2):160–72.

56. Dogan A, Ozdemir A, Kubar A, Oygür T. (2002). Assessment of periodontal healing by seeding of fibroblast-like cells derived from regenerated periodontal ligament in artificial furcation defects in a dog: a pilot study. Tissue Eng, 8(2):273–82.

57. Dan H, Vaquette C, Fisher AG, Hamlet SM, Xiao Y, Hutmacher DW, Ivanovski S. (2014). The influence of cellular source on periodontal regeneration using calcium phosphate coated polycaprolactone scaffold supported cell sheets. Biomaterials, 35(1):113-22.

58. Isaka J, Ohazama A, Kobayashi M, Nagashima C, Takiguchi T, Kawasaki H, Tachikawa T, Hasegawa K. (2001). Participation of periodontal ligament cells with regeneration of alveolar bone. J Periodontol, 72(3):314-23.

59. Tassi SA, Sergio NZ, Misawa MYO, Villar CC. (2017). Efficacy of stem cells on periodontal regeneration: Systematic review of pre-clinical studies. J Periodontal Res, 52(5):793–812.

60. Ding G, Liu Y, Wang W, Wei F, Liu D, Fan Z, An Y, Zhang C WS. (2010). Allogeneic periodontal ligament stem cell therapy for periodontitis in swine. Stem Cells, 28(10):1829–38.

61. Tsumanuma Y, Iwata T, Kinoshita A, Washio K, Yoshida T, Yamada A, Takagi R, Yamato M, Okano T, Izumi Y. (2016). Allogeneic Transplantation of

Periodontal Ligament-Derived Multipotent Mesenchymal Stromal Cell Sheets in Canine Critical-Size Supra-Alveolar Periodontal Defect Model. Biores Open Access, 1;5(1):22-36.

62. Zhu B, Liu W, Zhang H, Zhao X, Duan Y, Li D, Jin Y. (2017). Tissue-specific composite cell aggregates drive periodontium tissue regeneration by reconstructing a regenerative microenvironment. J Tissue Eng Regen Med, 11(6):1792-1805.

63. Nuñez J, Sanz-Blasco S, Vignoletti F, Muñoz F, Arzate H, Villalobos C, Nuñez L, Caffesse RG, Sanz M. (2012). Periodontal regeneration following implantation of cementum and periodontal ligament-derived cells. J Periodontal Res, 47(1):33-44.

64. Gao ZH, Hu L, Liu GL, Wei FL, Liu Y, Liu ZH, Fan ZP, Zhang CM, Wang JS, Wang SL. (2016). Bio-Root and Implant-Based Restoration as a Tooth Replacement Alternative. J Dent Res, 95(6):642-9.

65. Verrier S, Pallu S, Bareille R, Jonczyk A, Meyer J, Dard M, Amédée J. (2002). Function of linear and cyclic RGD-containing peptides in osteoprogenitor cells adhesion process. Biomaterials, 23(2):585-96.

66. Gilmore AP, Metcalfe AD, Romer LH, Streuli CH. (2000). Integrin-mediated survival signals regulate the apoptotic function of Bax through its conformation and subcellular localization. J Cell Biol, 149(2):431–45.

67. Kusindarta DL, Wihadmadyatami H. (2018). The Role of Extracellular Matrix in Tissue Regeneration. Tissue Regen.2018

68. Hynes RO. (2009). The extracellular matrix: not just pretty fibrils. Science, 326(5957):1216-1219.

69. Hynes RO. (1992). Integrins: Versality, Modulation, and Signaling in Cell Adhesion. Cell, 69(April):11–25.

70. Humphries JD, Byron A, Humphries MJ. (2006) Integrin ligands at a glance. J Cell Sci, 119(19):3901–3.

71. Ruoslahti E. (1996). RGD and Other Recognition Sequences for Integrins. Annu Rev Cell Dev Biol, 12(1):697–715.

72. Albelda SM, Buck CA. (1990). Integrins and other cell adhesion molecules. FASEB J, 4(11):2868-80.

73. Legate KR, Wickström SA, Fässler R. (2009). Genetic and cell biological analysis of integrin outside-in signaling. Genes Dev, 23(4):397–418.

74. Calderwood DA, Shattil SJ, Ginsberg MH. (2000). Integrins and actin filaments: Reciprocal regulation of cell adhesion and signaling. J Biol Chem, 275(30):22607–10.

75. Lebaron RG, Athanasiou KA. (2000). Extracellular Matrix Cell Adhesion Peptides : Functional Applications in Orthopedic Materials, 6(2):85–103.

76. Cary LA, Han DC, Guan JL. (1999). Integrin-mediated signal transduction pathways. Histol Histopathol, 14(3):1001–9.

77. Plow EF, Haas TA, Zhang L, Loftus J, Smith JW. (2000) Ligand binding to integrins. J Biol Chem, 275(29):21785–8.

78. Harburger DS, Calderwood DA. (2009). Integrin signalling at a glance. J Cell Sci, 122(9):1472.

79. Pierschbacher MD, Ruoslahti E. (1984). Cell attachment activity of fibronectin can be duplicated by small synthetic fragments of the molecule. Nature, 309(5963):30–3.

80. Pierschbacher MD, Ruoslahti E. (1984). Variants of the cell recognition site of fibronectin that retain attachment-promoting activity. Proc Natl Acad Sci U S A, 81(19 I):5985–8.

81. Yamada KM, Kennedy DW. (1987). Peptide inhibitors of fibronectin, laminin, and other adhesion molecules: Unique and shared features. J Cell Physiol, 130(1):21–8.

82. Hynes RO. (1993). Integrins: a family of cell adhesion receptors. Medicina (B Aires), 53(4):357–63.

83. Pfaff M. Recognition sites of integrins, within their ligands. In Springer, Boston, MA; 1997. p. 101–21.

84. Alipour M, Baneshi M, Hosseinkhani S, Mahmoudi R, Jabari Arabzadeh A, Akrami M, Mehrzad J, Bardania H. (2020). Recent progress in biomedical applications of RGD-based ligand: From precise cancer theranostics to biomaterial engineering: A systematic review. J Biomed Mater Res A, 108(4):839-850.

85. Wang F, Li Y, Shen Y, Wang A, Wang S, Xie T. (2013). The functions and applications of RGD in tumor therapy and tissue engineering. Int J Mol Sci, 14(7):13447–62.

86. Hersel U, Dahmen C, Kessler H. (2003). RGD modified polymers: Biomaterials for stimulated cell adhesion and beyond. Biomaterials, 24(24):4385–415.

87. Bellis SL. (2011). Advantages of RGD peptides for directing cell association with biomaterials. Biomaterials, 32(18):4205-10.

88. Boxus T, Touillaux R, Dive G, Marchand-Brynaert J. (1998). Synthesis and evaluation of RGD peptidomimetics aimed at surface bioderivatization of polymer substrates. Bioorganic Med Chem, 6(9):1577–95.

89. Groß A, Hashimoto C, Sticht H, Eichler J. (2016). Synthetic Peptides as Protein Mimics. Front Bioeng Biotechnol, 19;3:211.

90. Galli D, Benedetti L, Bongio M, Maliardi V, Silvani G, Ceccarelli G, Ronzoni F, Conte S, Benazzo F, Graziano A, Papaccio G, Sampaolesi M, De Angelis MG. (2011). In vitro osteoblastic differentiation of human mesenchymal stem cells and human dental pulp stem cells on poly-L-lysine-treated titanium-6-aluminium-4-vanadium. J Biomed Mater Res A, 97(2):118-26.

91. Bogdanowich-Knipp SJ, Chakrabarti S, Williams TD, Dillman RK, Siahaan TJ. (1999). Solution stability of linear vs. cyclic RGD peptides. J Pept Res, 53(5):530–41.

92. Markó K, Ligeti M, Mezo G, Mihala N, Kutnyánszky E, Kiss E, Hudecz F, Madarász E. (2008). A novel synthetic peptide polymer with cyclic RGD motifs

supports serum-free attachment of anchorage-dependent cells. Bioconjug Chem, 19(9):1757-66.

93. Marko K, Kohidi T, Nora H, Marta J, Gabor M, Madarasz E. (2011). Isolation of radial glia-like neural stem cells from fetal and adult mouse forebrain via selective adhesion to a novel adhesive peptide-conjugate. PLoS One, 6(12).

94. Tátrai P, Sági B, Szigeti A, Szepesi A, Szabó I, Bősze S, Kristóf Z, Markó K, Szakács G, Urbán I, Mező G, Uher F, Német K. (2013). A novel cyclic RGD-containing peptide polymer improves serum-free adhesion of adipose tissue-derived mesenchymal stem cells to bone implant surfaces. J Mater Sci Mater Med, 24(2):479-88.

95. Müller G, Kramer A. (2008). Biocompatibility index of antiseptic agents by parallel assessment of antimicrobial activity and cellular cytotoxicity. J Antimicrob Chemother, 61(6):1281–7.

96. Kanjevac T, Sekulic M, Radovic M, Vlaskovic A, Acovic A. (2017). Cytotoxic effects of three different oral antiseptic solutions on epithelial cells of buccal mucosa. Mediterr J Biosci, 1(5):192–6.

97. Müller HD, Eick S, Moritz A, Lussi A, Gruber R. (2017). Cytotoxicity and Antimicrobial Activity of Oral Rinses In Vitro. Biomed Res Int, 2017:4019723

98. Bowen J, Cole C, Mcglennen RC. (2015). Comparison of Antimicrobial and Wound Healing Agents on Oral Fibroblast Viability and In-vivo Bacterial Load. Dentistry 3000, 5:1-6.

99. De Oliveira JR, Belato KK, De Oliveira FE, Jorge AOC, Camargo SEA, De Oliveira LD. (2018). Mouthwashes: An in vitro study of their action on microbial biofilms and cytotoxicity to gingival fibroblasts. Gen Dent, 66(2):28–34.

100. Song I-S, Lee JE, Park J-B. (2019). The effects of various mouthwashes on osteoblast precursor cells. Open Life Sci, 14(1):376–83.

101. Tu Y-Y, Yang C-Y, Chen R-S, Chen M-H. (2015). Effects of chlorhexidine on stem cells from exfoliated deciduous teeth. J Formos Med A, 114(1):17–22.

102. Solderer A, Kaufmann M, Hofer D, Wiedemeier D, Attin T, Schmidlin PR. (2019). Efficacy of chlorhexidine rinses after periodontal or implant surgery: a systematic review. Clin Oral Investig, 23(1):21-32.

103. Wade WG, Addy M. (1989). In vitro Activity of a Chlorhexidine–Containing Mouthwash Against Subgingival Bacteria. J Periodontol, 60(9):521–5.

104. Hyamacharan D, Samanth A, Sheeja D, Varghese S. (2017). The Most Effective Concentration of Chlorhexidine as a Mouthwash-Systematic Review. S J. Pharm. Sci. & Res, 9(2):233–6.

105. Volpe AR, Kupczak LJ, Brant JH, King WJ, Kestenbaum RC, Schlissel HJ. (1969). Antimicrobial Control of Bacterial Plaque and Calculus and the Effects of these Agents on Oral Flora. J Dent Res, 48(5):832–41.

106. Haps S, Slot DE, Berchier CE, Van der Weijden GA. (2008). The effect of cetylpyridinium chloride-containing mouth rinses as adjuncts to toothbrushing on plaque and parameters of gingival inflammation: a systematic review. Int J Dent Hyg, 6(4):290–303.

107. Teng F, He T, Huang S, Bo CP, Li Z, Chang JL, Liu JQ, Charbonneau D, Xu J, Li R, Ling JQ. (2016). Cetylpyridinium chloride mouth rinses alleviate experimental gingivitis by inhibiting dental plaque maturation. Int J Oral Sci, 29;8(3):182-90.

108. Asadoorian J, Williams KB. (2008). Cetylpyridinium Chloride Mouth rinse on Gingivitis and Plaque. J Dent Hyg, 82(5):1–5.

109. Sreenivasan PK, Haraszthy VI, Zambon JJ. (2013). Antimicrobial efficacy of 0·05% cetylpyridinium chloride mouthrinses. Lett Appl Microbiol, 56(1):14–20.

110. Pires JR, Rossa Junior C, Pizzolitto AC. (2007). In vitro antimicrobial efficiency of a mouthwash containing triclosan/gantrez and sodium bicarbonate. Braz Oral Res, 21(4):342–7.

111. Glaser A. (2004). The Ubiquitous Triclosan A common antibacterial agent exposed. Pesticides and You, 24(3):12–7.

112. Zuckerbraun HL, Babich H, May RJ, Sinensky MC. (1998). Triclosan : cytotoxicity, mode of action, and induction of apoptosis in human gingival cells in vitro. Eur J Oral Sci, 106(16):628–36.

113. Wolf KJ. (2017). Safety and Effectiveness of Health Care Antiseptics; Topical Antimicrobial Drug Products for Over-the-Counter Human Use. Final rule. Fed Regist, 82(242):60474–503.

114. Greenstein G. (1999). Povidone-Iodine's Effects and Role in the Management of Periodontal Diseases: A Review. J Periodontol, 70(11):1397–405.

115. Zamora JL. (1986). Chemical and microbiologic characteristics and toxicity of povidone-iodine solutions. Am J Surg, 151(3):400–6.

116. Roche Diagnostics GmbH. RTCA SP Instrument Operator's Manual. (2009). 1–60.

117. Grimm W, Becher S, Varga G. (2011). The Ability of Human Periodontium-Derived Stem Cells to Regenerate Periodontal Tissues : A Preliminary In Vivo Investigation. Int J Periodontics Restor Dent, 31(6):94–101.

118. Karamzadeh R, Eslaminejad MB, Aflatoonian R. (2012). Isolation, characterization and comparative differentiation of human dental pulp stem cells derived from permanent teeth by using two different methods. J Vis Exp, (69):2–3.

119. Sekiya I, Larson BL, Vuoristo JT, Cui JC, Prockop DJ. (2004). Adipogenic Differentiation of Human Adult Stem Cells From Bone Marrow Stroma (MSCs). J Bone Min Res, 19(2):256–64.

120. Giaever I, Keese CR. (1984). Monitoring fibroblast behavior in tissue culture with an applied electric field. Proc Natl Acad Sci U S A, 81(12 I):3761–4.

121. Giaever I, Keese CR. (1991). Micromotion of mammalian cells measured electrically. Proc Natl Acad Sci U S A, 88(17):7896–900.

122. AECA Biosciences. Real-Time and Dynamic Monitoring of Cell Proliferation and Viability for Adherent Cells, 2013:1-8.

123. Brunner D, Frank J, Appl H, Schöffl H, Pfaller W, Gstraunthaler G. (2010). Serum-free cell culture: the serum-free media interactive online database. ALTEX, 27(1):53–62.

124. Gibon E, Batke B, Jawad MU, Fritton K, Rao A, Yao Z, Biswal S, Gambhir SS, Goodman SB. (2012). MC3T3-E1 osteoprogenitor cells systemically migrate to a bone defect and enhance bone healing. Tissue Eng Part A, 18(9-10):968-73.

125. Perczel-Kovách K, Hegedűs O, Földes A, Sangngoen T, Kálló K, Steward MC, Varga G, Nagy KS. (2021). STRO-1 positive cell expansion during osteogenic differentiation: A comparative study of three mesenchymal stem cell types of dental origin. Arch Oral Biol, 122:104995.

126. Goodman S, Holzemann G, Sulyok G, Kessler H. (2002). Nanomolar Small Molecule Inhibitors for avb6, avb5, and avb3 Integrins. J Med Chem, 45:1045–51.

127. Tsuji K, Ojima M, Otabe K, Horie M, Koga H, Sekiya I, Muneta T. (2017). Effects of Different Cell-Detaching Methods on the Viability and Cell Surface Antigen Expression of Synovial Mesenchymal Stem Cells. Cell Transplant, 26(6):1089-1102.

128. Angstmann M, Brinkmann I, Bieback K, Breitkreutz D, Maercker C. (2011). Monitoring human mesenchymal stromal cell differentiation by electrochemical impedance sensing. Cytotherapy, 13(9):1074-89.

129. Nordberg RC, Zhang J, Griffith EH, Frank MW, Starly B, Loboa EG. (2017). Electrical Cell-Substrate Impedance Spectroscopy Can Monitor Age-Grouped Human Adipose Stem Cell Variability During Osteogenic Differentiation. Stem Cells Transl Med, 6(2):502-511.

130. Bagnaninchi PO, Drummond N. (2011). Real-time label-free monitoring of adipose-derived stem cell differentiation with electric cell-substrate impedance sensing. Proc Natl Acad Sci U S A, 108(16):6462-7.

131. Hagi-Pavli E, Williams DM, Rowland JL, Thornhill M, Cruchley AT. (2014). Characterizing the immunological effects of oral healthcare ingredients using an

in vitro reconstructed human epithelial model. Food Chem Toxicol, 74:139-48

132. Wyganowska-Swiatkowska M, Kotwicka M, Urbaniak P, Nowak A, Skrzypczak-Jankun E, Jankun J. (2016). Clinical implications of the growth-suppressive effects of chlorhexidine at low and high concentrations on human gingival fibroblasts and changes in morphology. Int J Mol Med, 37(6):1594–600.

133. Goldschmidt P, Cogen R, Taubman S. (1977 Cytopathologic Effects of Chlorhexidine on Human Cells. J Periodontol, 48(4):212–5.

134. Peacock ME, Sutherland DE, Schuster GS, Brennan WA, O'Neal RB, Strong SL, et al. The Effect of Chlorhexidine Treatment Human Gingival Fibroblasts In Vitro. J Periodontol. 1991;62(7):434–8.

135. Liu JX, Werner J, Kirsch T, Zuckerman JD, Virk MS. (2018). Cytotoxicity evaluation of chlorhexidine gluconate on human fibroblasts, myoblasts, and osteoblasts. J Bone Jt Infect, 3(4):165-172.

136. Lee TH, Hu CC, Lee SS, Chou MY, Chang YC. (2010). Cytotoxicity of chlorhexidine on human osteoblastic cells is related to intracellular glutathione levels. Int Endod J, 43(5):430–5.

137. Lessa FC, Aranha AM, Nogueira I, Giro EM, Hebling J, Costa CA. (2010). Toxicity of chlorhexidine on odontoblast-like cells. J Appl Oral Sci, 18(1):50-8.

138. Cline N V., Layman DL. (1992). The Effects of Chlorhexidine on the Attachment and Growth of Cultured Human Periodontal Cells. J Periodontol, 63(7):598–602.

139. Chang YC, Huang FM, Tai KW, Chou MY. (2001). The effect of sodium hypochlorite and chlorhexidine on cultured human periodontal ligament cells. Oral Surg Oral Med Oral Pathol Oral Radiol Endod, 92(4):446-50.

140. Hidalgo E, Dominguez C. (2001). Mechanisms underlying chlorhexidine-induced cytotoxicity. Toxicol Vitr, 15(4–5):271–6.

141. Fernández E, Sánchez MDC, Llama-Palacios A, Sanz M, Herrera D. (2017). Antibacterial Effects of Toothpastes Evaluated in an In Vitro Biofilm Model. Oral Health Prev Dent, 15(3):251-257

142. Riley P, Lamont T. Triclosan/copolymer containing toothpastes for oral health. Cochrane Database Syst Rev, 2013(12).

143. Park BK, Gonzales ELT, Yang SM, Bang M, Choi CS, Shin CY. (2016). Effects of triclosan on neural stem cell viability and survival. Biomol Ther, 24(1):99–107.

144. Schmidlin PR, Imfeld T, Sahrmann P, Tchouboukov A, Weber FE. (2009). Effect of Short-Time Povidone-Iodine Application on Osteoblast Proliferation and Differentiation. Open Dent J, 3:208–12.

## 10. BIBLIOGRAPHY OF THE CANDIDATE


1. **Khorolsuren Zambaga**, Lang Orsolya, Pallinger Eva, Foldes Anna, Gyulai-Gaál Szabolcs, Varga Gabor, Mezo Gabor, Vag Janos, Kohidai Laszlo
   Functional and cell surface characteristics of periodontal ligament cells (PDLCs) on RGD-synthetic polypeptide conjugate coatings. JOURNAL OF PERIODONTAL RESEARCH 55: 5 pp. 713-723. (2020). DOI: 10.1111/jre.12760

2. **Khorolsuren Zambaga**, Lang Orsolya, Vag Janos, Kohidai Laszlo
   Effect of dental antiseptic agents on the viability of human periodontal ligament cells. SAUDI DENTAL JOURNAL. (2021). DOI: 10.1016/j.sdentj.2021.09.016

## 11. ACKNOWLEDGEMENTS

Firstly, I would like to sincerely thank my supervisors Professor László Kőhidai and Professor János Vág, for their guidance and mentorship and for the opportunity to learn about science and challenge my potential during my Ph.D. experience.

Special thanks to Dr. Orsolya Láng for her patience and guidance in setting up my projects.

My sincere thanks go to Prof. Gábor Mező for the synthetic materials he provided us kindly.

I would like to thank Dr. Anna Földes for her help and teaching on cell isolation and PCR technique, and also to Dr. Éva Pállinger for her kind assistance on flow cytometry analysis. Thank you, Dr. Eszter Lajkó, for always encouraging me and giving me helpful, practical tips in laboratory works.

I would like to express my gratitude for the financial support received from the Stipendium Hungaricum Tempus Public Foundation and the Hungarian scientific research fund (K112364), the Faculty of Dentistry research fund (2016), and the Doctoral School for funding my attendance at some unforgettable conferences.

Thank you, my friends, especially Sundi and Uyanga, for always being on my side and encouraging me. Thank you, Noni, my sweet little niece, for being here with me.

I am most grateful to my whole lovely family, especially my mom and dad, for always supporting and inspiring me.